

Vertical stress profiles and the significance of “stress decoupling”

François H. Cornet⁽¹⁾ and Thomas Röckel⁽²⁾

(1) Institut de Physique du Globe de Strasbourg,- CNRS ; 5 rue René Descartes 67 000
Strasbourg, France ; françois.cornet@unistra.fr

(2) Piewak & partner Gmbh ; Jean Paul Strasse 30 ; 95444 Bayreuth, Germany,
thomas.roeckel@piewak.de

Abstract

Precise determinations of the complete stress tensor have been conducted at various depths near the village of Bure, in the eastern part of the Paris sedimentary Basin. They show that the magnitude of the principal stress components do not vary linearly with depth for this site. Similarly, precise data on the variation with depth of the maximum horizontal principal stress orientation, both in the southern Rhine Graben and in the North German Basin, vary significantly with depth. Vertical variations are controlled by the rheological characteristics and the relative thickness of the various formations. Hence the stress field observed at shallow depths in sedimentary formations may be decoupled from that which prevails at greater depth. It is proposed that in domains of very slow deformation rates, local deformation processes possibly associated with rock-fluid interactions, but also with diapirism, may influence more significantly the local stress field than does the regional tectonic activity. Further, because principal stress directions have been found to rotate with depth both in sedimentary rocks as well as in crystalline and metamorphic domains down to depth much larger than those associated with topographic effects, it is concluded that large scale stress field analyses must take into account depths at which the various data have been collected.

1. Introduction

Jacques Angelier has always been a strong promoter for applying principles of mechanics to structural geology. In 2005 a special session on regional stress field characterization was organized at the annual meeting of the European Geophysical Union during which Jacques gave an invited talk on this topic. The object of the present paper is to follow up on the discussion about stress decoupling in sedimentary basins that took place during this meeting, as a tribute to Jacques's contribution to understanding stress fields in geological materials at various scales.

It is often considered that, at a multi kilometre scale in the upper crust, the magnitudes of the principal stress components vary linearly with depth independently of rock type (e.g. Brace and Koelstedt, 1980; Zoback et al., 2003). This linear variation is often taken as a demonstration that the upper crust is very close to failure and that failure is controlled by slip on optimally oriented pre-existing faults.

Yet, at the scale of tens of meters, it is well known in the oil industry that within sedimentary formations the vertical gradient of the minimum horizontal principal stress does not vary linearly with depth. This is well demonstrated by the limited vertical extension of hydraulic fractures that propagate horizontally over distances larger than a few hundred meters in stratified formations (e.g. Economides & Nolte, 2003). Because generally the minimum horizontal principal stress magnitude is smaller in stiff rocks like limestone or sandstone than it is in the clay rich materials that are underlying and overlying the stiff formations, hydraulic fractures remain confined within the stiffest formations. This has been often confirmed through microsismic monitoring of large (100 m scale) hydraulic fracture propagation (e.g. Rutledge and Philips, 2003; Sileny et al., 2009).

It has long been considered that these non linear variations of the minimum principal stress are linked to variations in the elastic constants of the geomaterials (e.g. Anderson et al., 1973). But Thiercelin and Plumb (1994) showed that models derived from elasticity considerations and models derived from failure considerations yield somewhat similar results, given the uncertainties associated with the model parameters evaluation.

In this paper we present detailed observations on vertical stress variations within sedimentary formations. This helps outlining the influence of the rheological characteristics of geomaterials on vertical stress profiles. It demonstrates the occurrence of so called "stress decoupling" through very soft geomaterials.

The first example refers to a complete stress determination that was conducted within and around a 150 m thick clay rich layer in the Eastern Paris Basin, in France. The volume that has been investigated extends over an area about 100 km², within a depth range that varies from 300 m to 750 m. Then we turn to the effect of salt deposits on regional stress fields and discuss results from the southern upper Rhine graben as well as from various different sites in the northern German Basin, some of which are more than 5 km deep. Results at depths greater than 4 km and below the Zechstein deposit are then compared to those obtained in boreholes drilled below 4 km in four different crystalline and metamorphic sites.

These examples illustrate the effect of differential stress relaxation through the weaker rocks, both on principal stress magnitudes (Paris Basin) and on principal stress directions (Rhine graben, northern German basin). They demonstrate the limits of the classical assumption on linear variation with depth of principal stress magnitudes for sedimentary formations subject to very slow deformation rates. More generally they raise questions on the significance of methods used for upscaling local observations when considering natural stress fields and on the relevance of considering superficial stress fields for discussing plate tectonics or seismic hazard issues in such very slow deforming zones.

2. Influence of clay rich layers on vertical stress profiles – a case history from the eastern Paris Basin

For the last fifteen years, ANDRA, the French radioactive waste management agency, has been investigating the possibility of developing a long term repository in the eastern Paris Basin, near the small village of Bure (Haute Marne). There, the targeted 150 m thick Callovo-Oxfordian (COX) clay rich layer (argillite) is interbedded between the 224 m thick Dogger limestone (below) and the 212 m thick Oxfordian limestone (above), all of which are sub-horizontal (dip smaller than 3 degrees). Design of a potential repository requires an accurate determination of the complete natural stress field within the argillite formation and its surrounding.

A first set of measurements was conducted in the immediate vicinity of the Underground Research Laboratory (URL) that has been developed for undertaking the required in situ testing. This stress determination relied on hydraulic tests in boreholes including both classical Hydraulic Fractures (HF) and Hydraulic Tests on Pre-existing Fractures (HTPF) (see Haimson and Cornet, 2003, for description of HF and HTPF tests). Vertical, inclined and horizontal boreholes have been taken to advantage so that axial and en-echelon fractures have been analyzed for a precise evaluation of the orientations and magnitudes of all three principal stress components.

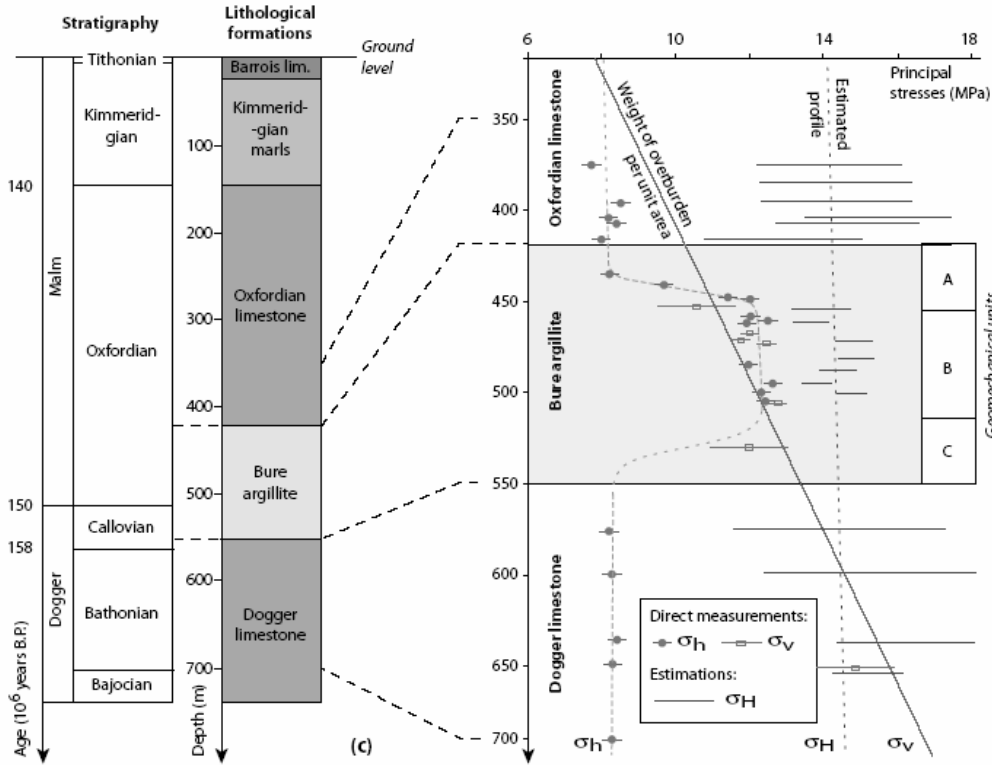


Figure 1. Results from the complete stress determination at the Underground Research Laboratory (URL), in the Eastern Paris Basin (Gunzburger and Cornet, 2007; Wileveau et al., 2007).

While the mud used in most drilling operations is usually prepared with water, in clay rich formations mud may be prepared with hydro-carbons in order to prevent weakening effects associated with clay-water interactions. At Bure, boreholes have been drilled with both, water based mud and oil based mud. It has been observed that borehole breakouts (see

Zoback et al., 2003, for the definition of borehole breakouts and their use for constraining some of the stress field components) have always developed in boreholes drilled with water based mud but have not been observed in boreholes drilled with oil based mud. Laboratory results (ANDRA, 2007) have showed that cores collected with oil based mud were stronger than cores collected with water based mud (differences in uniaxial compressive strength vary from 6 to 28 MPa, depending on sampling location within the COX strata). Because the compressive strength of argillite formations intersected by boreholes depends on whether the borehole has been drilled with oil based mud (stronger) or with water based mud (weaker), the appearance or non appearance of borehole breakouts has been used to define upper bounds and lower bounds to the maximum horizontal principal stress magnitude.

Finally, these stress data have been validated by the modeling of the convergence measured during the sinking of the vertical shaft used for accessing the underground laboratory (see Wileveau et al., 2007, or Cornet, 2010, for a detailed discussion on these methods and results). Results obtained at the URL site are summarized in figure 1.

Figure 1 integrates in addition to the results from URL, those from an inclined well (EST312, on fig. 2) that was drilled some 15 km from URL and that reached the Dogger formation below the argillite. The large error bar on the maximum horizontal principal stress amplitude for tests in the Dogger and Oxfordian limestone reflects the uncertainty on the influence of pore pressure on breakdown pressure interpretation for HF tests (limits of the error bars correspond to correcting or not correcting for pore pressure effects in the breakdown equation).

Then additional measurements were undertaken in order to investigate lateral variations of the various COX formation characteristics, including the stress field. Locations of the various sites where data have been collected are shown on figure 2 together with the main geological structures. Further, a shaft has been drilled over the initial EST205 vertical borehole used for the initial stress measurements at URL. It has brought some new information on orientation of fractures created during these initial HF tests.

Boreholes where data have been collected are distributed in three main sites that correspond roughly to the summits of a 15 km sided equilateral triangle within the green curve shown on figure 2. One summit is located to the south, on the Underground Research Laboratory (URL); one summit is located to the north-east of the URL (boreholes EST312 and EST413) and one to the north west of it (boreholes EST441 and MSE101). The investigated area is about 100 km². The thickness of the calovo-oxfordian (COX) argillite formation varies from about 140 m at the URL, to about 160 m at the north-east site and 152 m at the north-west site.

Variability in the principal stress directions

Clear breakouts have been identified within the COX formation for all boreholes that were drilled with water based mud. Their mean direction is $N 60 \pm 15^\circ E$, completely consistent with the mean orientation of the mean Hydraulic Fracture orientations ($N 151^\circ E$) obtained for thirty different tests distributed in the various boreholes (tables 1 and 2). Hence both sets of results indicate a very steady direction for the maximum horizontal principal stress component S_H .

A more detailed analysis reveals that in fact stress orientations are defined locally, at the 50 m scale, to better than 10° , but that they may vary in space by about 10 to 15° from one sedimentary layer to the other on the same site.

For most of the sites, Hydraulic Fractures are vertical but locally they appear to be slightly en echelon, suggesting that the vertical direction may be inclined locally by more than

15° from the corresponding principal direction, given the boreholes remain vertical to within 1 or 2°.

Hence these results outline a variability in the principal stress directions that may reach 15° at the scale of the site (100 km²), while the resolution of the methods indicate steady values (dispersion smaller than 7°) at the 50 m scale.

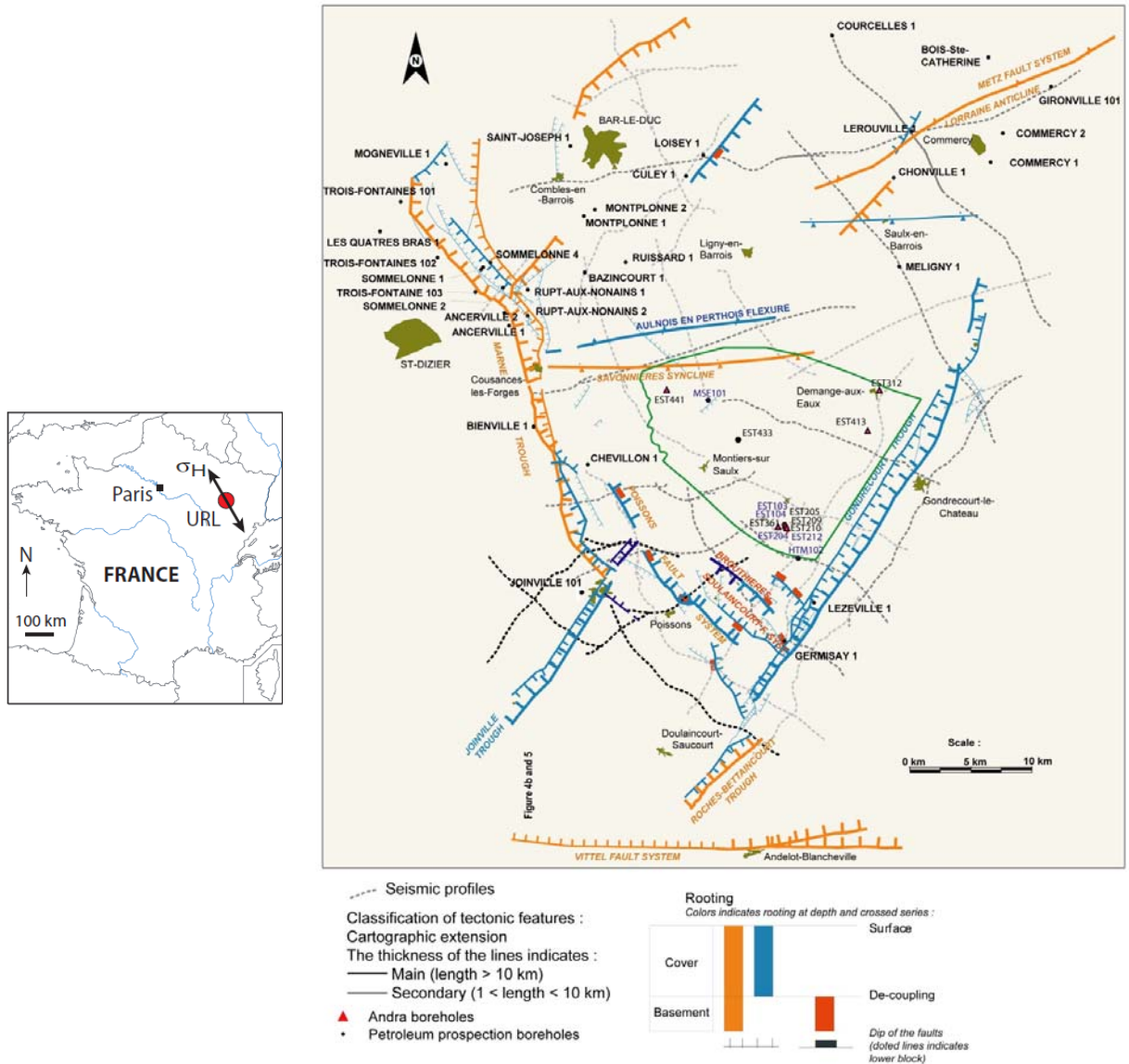


Figure 2: Stress observations have been recovered from the various boreholes located within the area delimited by the green contour line, with the URL site located where the density of boreholes is the highest (including EST205). The North East corner includes wells EST312 and EST413, whilst the North West corner includes wells EST441 and MSE2101. Orange coloured structures extend into the basement rock below the sedimentary cover while blue coloured ones remain within the sediments.

Variability in the vertical stress component

Efforts have been undertaken to measure directly the vertical stress component S_v through HTPF tests conducted on horizontal discontinuities between sedimentary beds. These measurements have been quite successful within the COX formation so that the mean vertical stress component was directly measured both at the URL site and for borehole EST413 at the north east site. In addition, when a shaft was sunk over the EST205 borehole used for the preliminary HF stress measurements, it revealed that some of the fractures that had been identified as being vertical from impression packers were found to have extended horizontally away from EST205 (Impression packers take oriented prints of borehole walls and are commonly used to identify Hydraulic Fracture (HF) orientations; Haimson and Cornet, 2003). Hence this gave direct evidence that the vertical stress component at these locations (table 3) is the minimum principal stress.

While all measurements are consistent with a vertical gradient of the vertical component equal to 0.0254 MPa/m for the URL site, they yield a value of 0.0234 MPa/m for the EST413 site. However the mean density of the deposit between the COX and ground surface as derived from direct laboratory density measurements yields a value equal to 0.0245 MPa/m.

Interestingly the EST413 well is located on the top of a plateau that dominates a river by about 130 m so that topography affects locally the magnitude of the vertical component. Corrections based on the elastic solution proposed by Savage et al. (1985) yield a mean vertical gradient equal to 0.025 MPa/m, quite consistent with anticipated values.

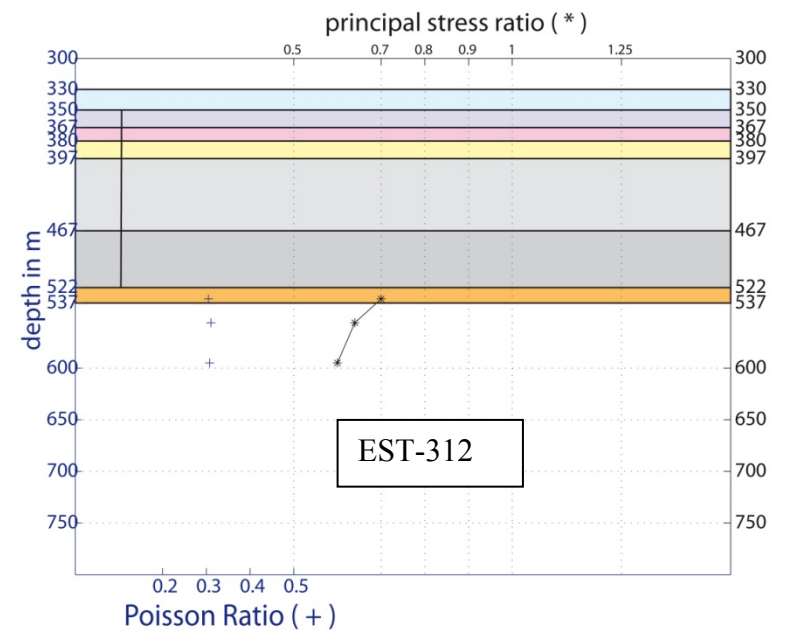
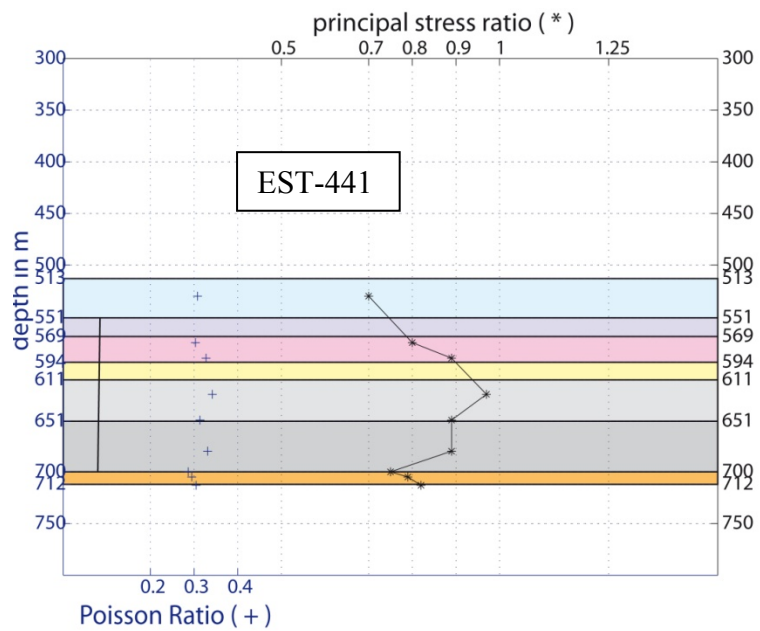
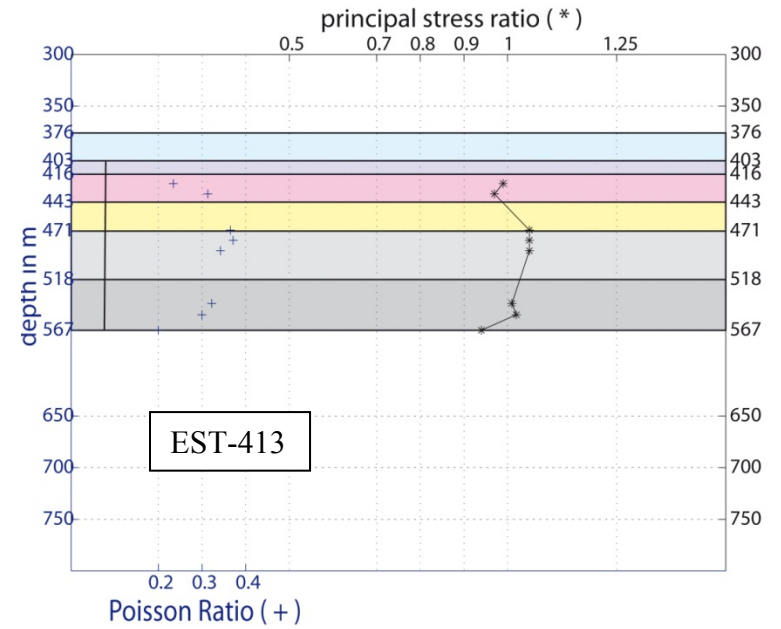
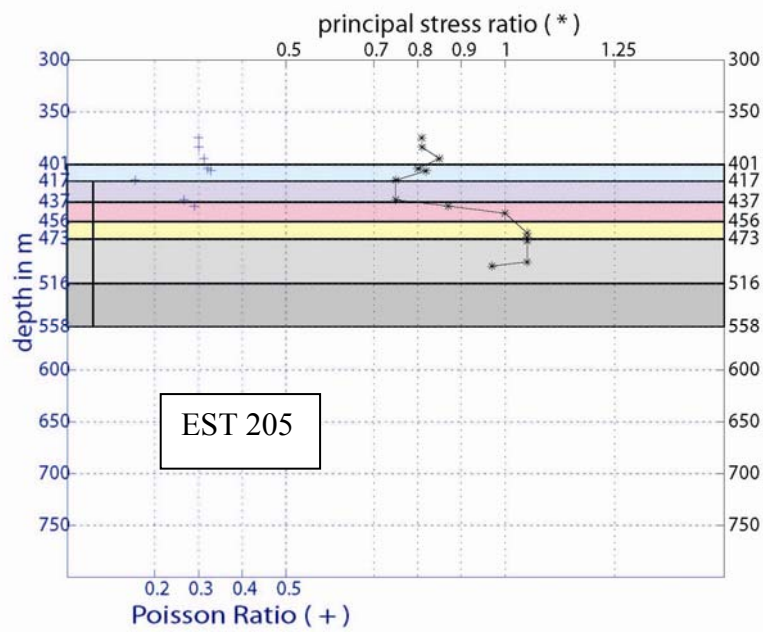


Figure 3. Vertical variation of Poisson's ratio and of the S_h/S_v ratio as a function of the sedimentary structure at the various sites. The vertical line, to the left of each diagram, indicates the COX formation vertical extension. The depth scale is the same for all diagrams so that variability in depth and in thicknesses of the various layers from one borehole to the other may be readily observed. Top left (borehole 205) corresponds to the Underground Research Lab (URL) in the southern corner of the investigated area; Lower left (EST-441) is located in the North-West corner of the investigated area ; Boreholes EST- 413 and EST-312 are located in the North East corner of the investigated area.

Variability in the S_h/S_v ratio

The various results for the minimum horizontal principal stress magnitudes S_h are presented in table 3. We plot on figure 3 variations with depth of the ratio between the measured minimum horizontal and the vertical principal stress magnitudes S_h/S_v . For borehole EST441 where no HTPF tests on subhorizontal fractures were conducted, the vertical component has been computed on the hypothesis that the vertical gradient is 0.025 MPa/m. We also plot the value of the dynamic Poisson's ratio as derived from sonic logs run in the same wells. Values shown in figure 3 correspond to the mean dynamic Poisson's ratio value determined over a 1 m borehole length.

While clearly the S_h/S_v ratio is the highest (and slightly above 1) where the Poisson's ratio is also the highest, details of the variation with depth of both quantities are not quite similar. The dynamic Poisson's ratio varies around 0.3 with some local values lower than 0.2. The S_h/S_v ratio is larger than 0.9 and is often close to 1 within the clay rich COX layers. It is smaller than 0.8 and gets as low as 0.6 within the calcite rich Oxfordian or Dogger layers even though, in this formation the dynamic Poisson's ratio is close to 0.3.

Constraints on the maximum horizontal principal stress component S_H

Only two well resolved values (better than 1 MPa) have been obtained for the S_H magnitude. It has been found equal to 13.9 MPa from an HTPF test run in the Oxfordian limestone at a depth of 520 m in well EST441 in the North West corner of the area of investigation. It has been found equal to 14 ± 1 MPa at a depth of 655 m from an echelon fractures observed in an inclined well on the URL site, within the Dogger limestone, in the South corner. Further, the absence or presence of breakouts in the COX formation between 440 m and 550 m, depending on whether the borehole had been drilled with water or oil based mud, provided means to conclude that S_H in this formation is equal to 15 ± 2 MPa.

The observation of well identified breakouts in wells drilled with water based mud clearly demonstrates that a significant difference exists between both horizontal stress magnitudes so that there is no doubt that S_H is larger than the vertical component S_v within and above the COX .

Discussion on the mechanisms that controls the present day stress field in the Paris Basin

It is concluded from the stress determination described here above that the maximum horizontal stress is larger than the vertical component above the COX but that the stress tensor is sub-isotropic (maximum value for the maximum differential stress smaller or equal to 2 MPa) for layers the richest in clay minerals within the COX. A question arises on the origin of this large maximum horizontal stress component above the COX.

Generally two sources of stress are considered, gravity related mechanisms and tectonics. In the absence of significant topographic effects (the deepest valley is less than 130 m deep with respect to the "plateau" structure of the area) and because the sedimentary layers are sub-horizontal (3° dip to the NW), a magnitude for S_H larger than that for S_v cannot be explained by simple gravity effects. As shown by Gunzburger and Cornet (2007), erosion and past glaciations may explain the large values for the horizontal stress components at ground surface but these effects yield axisymmetrical horizontal components, which are not consistent with observations.

Also, the Paris Basin is mostly constituted by plate shaped structures that outcrop on the borders of the basin. The absence of major faults with significant vertical offsets and the outcropping of the cretaceous and Jurassic formations raise difficulty to understand how horizontal tectonic stresses might be exerted onto the geological formations above the COX. Indeed, given the COX supports only a very small deviatoric stress because of its rheological properties, tectonic stresses are not transmitted to the more superficial layers.

Further, the complete absence of microseismicity in the Paris Basin (Grünthal and Wahlström, 2003, figure 4) and the absence of large scale horizontal motion as detected by GPS monitoring (Nocquet and Calais, 2004) indicate that no significant horizontal large scale active deformation process exists today in this area.

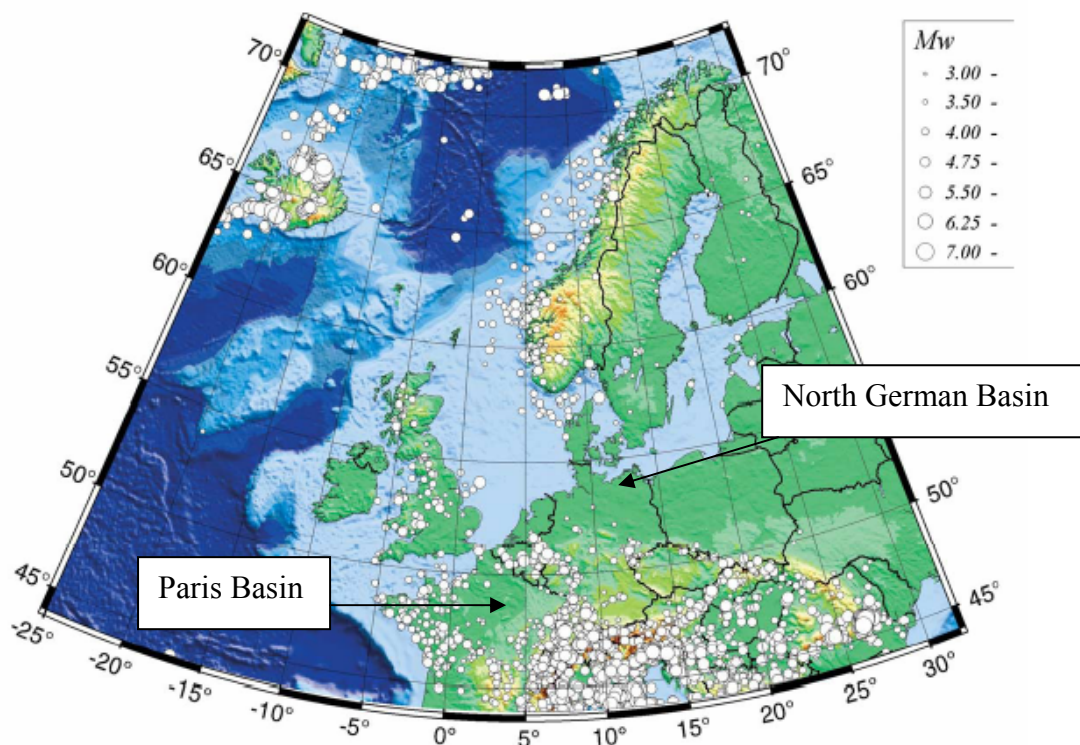


Figure 4. Microseismic activity in North-western Europe from 1300 till 1993 for microseismic events with magnitude M_w larger or equal to 3.5 (adapted from Grünthal and Wahlström, 2003)

The important conclusion here is that the natural stress field measured on a 100 km^2 area at depth ranging between 300 m and 700 m does not vary linearly with depth and is not controlled by friction on preexisting well oriented faults. Rather, the stress magnitudes seem to be controlled by the creeping characteristics of the various layers rather than by their elastic characteristics, with a loading mechanism that remains to be identified but which is neither related directly to gravity nor apparently to present tectonics.

While nearly no fractures have been identified in the COX, the distribution of fracture orientations identified within both the Dogger and the Oxfordian limestone exhibit a strong preferential orientation in the $N150^\circ E$ direction, i.e. parallel to the maximum horizontal stress direction (figure 5). This is completely consistent with the observation of fast shear wave arrivals in this same direction at various locations of the Paris Basin (Lefevre et al., 1992), as derived from Vertical Seismic Profiles. Interestingly, shear wave splitting has been observed both in the Dogger formation and at the top of the Kimmeridgian limestone as well as within the Albian sandstone while in between these layers a thick zone is found to be isotropic. This

zone includes the Callovo-Oxfordian layers and thus this measured isotropy is consistent with the observation that very little differential stresses are supported by the COX.

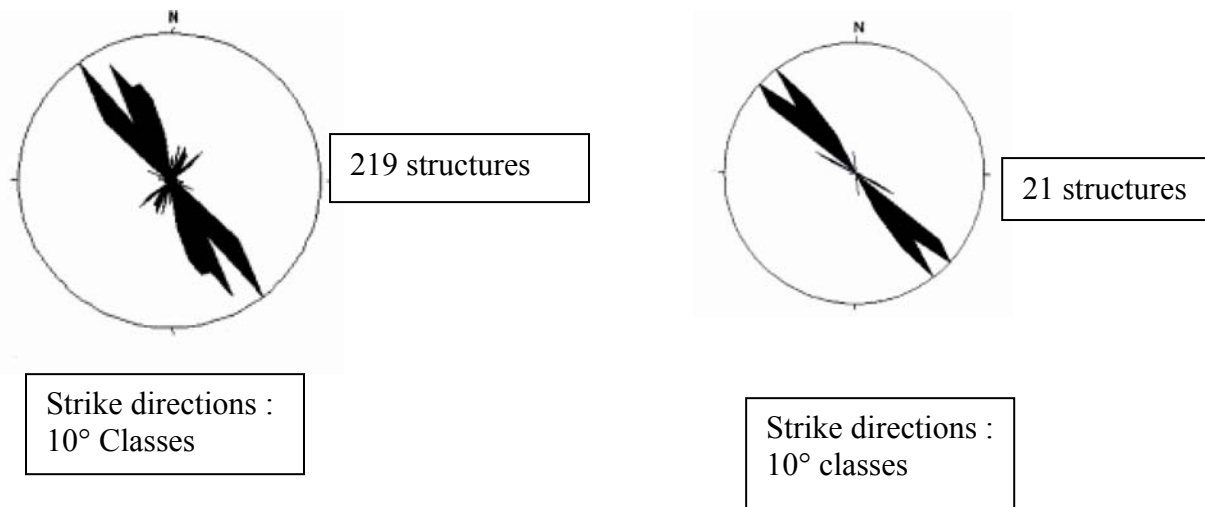


Figure 5. Orientations of joints and fractures in the Dogger limestone (left) and in the Oxfordian limestone (right).

The following hypothetical loading mechanism may be proposed: a preferential fracture orientation was developed during the Alpine tectonic orogeny some twenty million years ago, when this material was buried at greater depth and did not outcrop. Since then, fluid circulation at various scales but in the preferential fracture direction has resulted in some local dissolution of the fracture walls. This dissolution in a preferred direction led to a decrease in the stress component that is acting perpendicularly to the main fracture orientation. This proposed mechanism would be consistent with the absence of large scale displacement and would result in a decrease in the minimum horizontal principal stress magnitude within the limestone formations. The mechanism would still be active today therefore resulting in the present loading of the COX by the limestone. Some proper modeling must be conducted to substantiate this hypothesis. Preliminary results (Toussaint and Cornet, 2011) suggest that indeed this mechanism may yield the proper orders of magnitude for the observed difference in stress magnitudes. Furthermore, it would provide an explanation for the observed pore pressure parabolic profile measured within the COX (Delay et al., 2006).

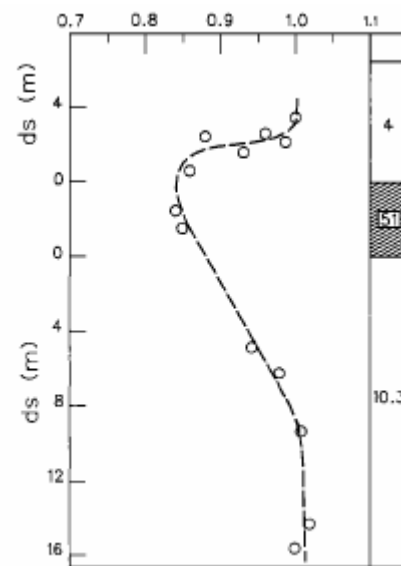
3. Evidence for stress decoupling in the upper Rhine Graben.

In 1992, Cornet and Burllet reported on stress measurements that had been conducted in a potash mine near Mulhouse, in the southern upper Rhine graben in France. On this site a large hydraulic fracture had been developed at a depth of 500 m for the purpose of testing solution mining. Later on, the fracture was mined out over a distance larger than 50 m and was found to be vertical and oriented in the N7°E direction. Interestingly this direction was also that of a still active salt diapir that outcrops along an about 10 km long zone at a distance of about 5 km from the site where the fracture has been generated. Later, various HF tests were conducted at depths ranging from 700 m to 950 m to determine the local stress field and it was found that the ratio between the magnitude of the minimum horizontal principal stress and that of the vertical component varied in a non linear manner depending on the anhydrite content of the formation (see figure 6).

But in 2005 a 5 km deep borehole was drilled in Basel, some 25 km away from the potash mine. The well was the site of numerous breakouts below 3km (Valley and Evans, 2009) and outlined a very clearly defined N150°E direction for the maximum horizontal principal stress. A somewhat similar S_H direction (N145°E) has been determined from an inversion of focal mechanisms of local micro-earthquakes (Plenefisch and Bonjer, 1997).

Hence, in the southern upper Rhine graben the principal stress directions observed in the basement rock differs by more than 30° from that measured in the sedimentary layers above it. Further in the sedimentary salt rich layers the stress magnitude variation with depth is found to be strongly non linear and directly linked to the anhydrite content. No attempt has been made at modelling the stress field within the sedimentary formation. Clearly such a modelling must involve diapirism of evaporitic formations, again a feature quite outside the scope of the present paper.

Figure 6 Variation of the S_h/S_v ratio (horizontal axis) as a function of the distance ds (in meters, vertical axis) to layer rich in anhydrite (51%). Numbers in the column to the right indicate the anhydrite content (in percent) in the different layers (after Cornet and Burlet, 1992)



It is only concluded here that, at this location, the principal stress magnitudes do not vary linearly with depth within the sedimentary cover. Further, the principal stress directions observed in the upper sediments are not representative of the regional tectonics even though no topographic effect exists in the area.

4. Evidence for stress decoupling in the Northern German Basin

4.1. Principal stress directions

Roth and Fleckenstein (2001) and Röckel and Lempp (2003) have reported strong differences in the principal stress directions observed above and below the basin wide Zechstein salt layer (figure 7) in the northern German Basin.

Their conclusion results from a compilation of borehole breakout orientations observed in a large collection of deep wells that intersect the Zechstein. Some of them reach depths larger than 6 km.

Interestingly, the mean S_H direction identified below the Zechstein salt layer seems to be roughly oriented in the N-S direction although it varies from N 30°E in the eastern part of the basin to the NW-SE direction (N135°E) in the westernmost part of the basin. This NW-SE direction is precisely the mean S_H direction often accepted for North Western Europe (Mueller et al., 1992; Zang and Stephansson, 2010).

It may be mentioned that diapirism of the Zechstein evaporitic formation is well documented (Tingay et al., 2006) and certainly affects the stress distribution within the sedimentary above the Zechstein unit.

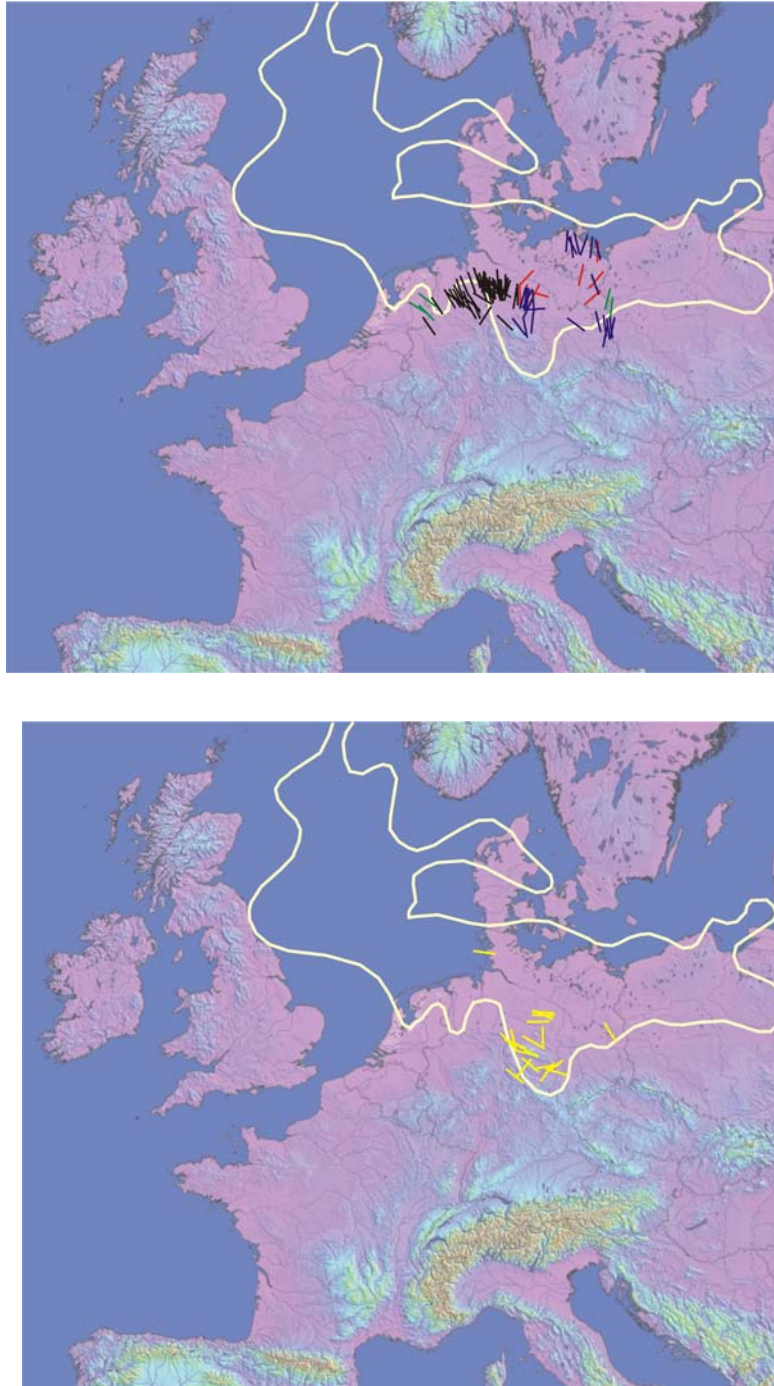
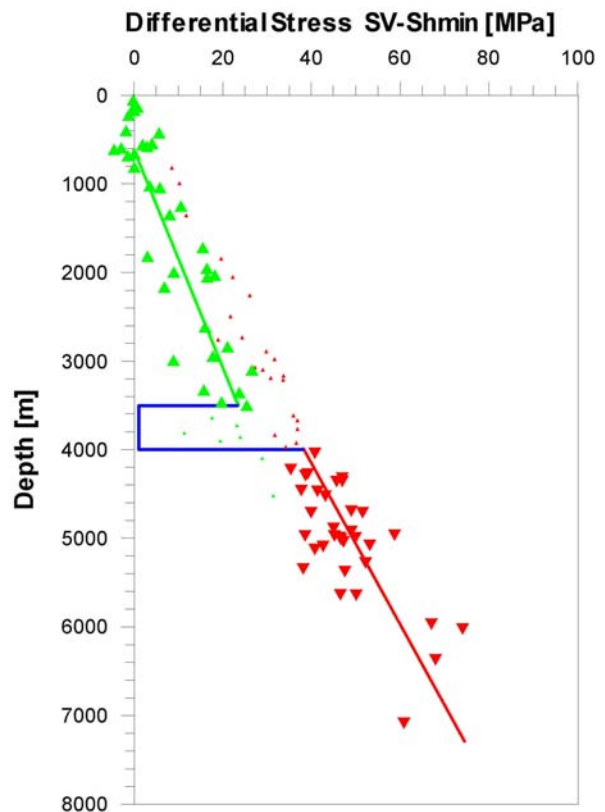


Figure 7. Maximum horizontal principal stress direction. *Top*, sub Zechstein salt data; Data from Grote (1998) are presented as white arrows, from Roth et al. (1998) and from Roth & Fleckenstein (2001) by red arrows, and the data from Röckel & Lempp (2003) in blue. Stress indicators at the WSM at the border of the Netherlands and Poland are presented in green. *Bottom*, supra Zechstein salt data (from Röckel and Lempp, 2003). The yellow contour indicates the limits of the Zechstein layer

4.2. Principal stress magnitudes

For most of the boreholes, the loss of drilling mud and results from leak-off tests (small Hydraulic Fracture tests conducted just below the casing, see Zoback et al., 2003, for definition of Leak-off tests) have provided data of the minimum horizontal principal stress magnitude. Also, the mean density for the various layers is well known (Barrio-Alvers et al., 1998) so that the vertical stress component may be estimated from the cumulated weight of overburden (Tables 4 to 7). This provides an estimate of the variation with depth of the maximum differential stress supported by the formation at depths where leak-off tests have been conducted. Results are summarized on figure 8.

Figure 8 Variation with depth of the (Sv-Sh) differential stress in the Eastern part of the North German basin. The blue notch between 3500 and 4000 m corresponds to the Zechstein evaporitic formation where the differential stress is found to drop for most of the boreholes. The dots correspond to either subsalt data (red) or suprasalt data (green) from boreholes at locations where the salt is either above or below the mean depth encountered in most of the wells. The gradient of the differential stress in the subsalt is higher compared with the gradient above the salt. Within the salt layer the gradient of the differential stress is close to zero.



The variation with depth of the maximum differential stress is found to be grossly equal to 6.5 MPa/km above the salt while it is 9.4 MPa/km below it. This implies that the Sh/Sv ratio varies from about 0.74 in the supra-salt layers to about 0.62 within the sub-salt layers.

Above the salt, the pore pressure has been found to be close to hydrostatic equilibrium. Below the salt, pore pressure has been measured in the Rotliegend formation (table 8). It is always above hydrostatic (compared with fresh water) and varies between 0.0106 MPa/m and 0.0122 MPa/m (brines very rich in salt) in the eastern part of the German basin but reaches 0.014 MPa/m at two sites close to the basin centre.

5. Discussion

5.1. Smoothing out stress magnitudes

Results from figure 3 showing the influence of clay content on the principal stress magnitudes at Bure, in the Paris Basin, may be plotted on a unique graph, in a manner

somewhat similar to that adopted for data from the North German basin. When doing so (figure 9), a grossly linear increase of S_h magnitude with depth is observed. When one plots the difference between the vertical and the minimum horizontal stress components, the slope of the linear trend defined by a least squares procedure yields a value of 7 MPa /km, somewhat similar to that identified in the North German Basin. The standard deviation on differences between the actual values and the linear regression is 1.4 MPa, i.e. it corresponds to errors ranging between 10 and 18 % of the individual values for S_h , depending on depth, while all uncertainties associated with the measurements were always smaller than 10%. Hence if one applies the classical hypothesis that vertical stress variation is controlled by friction on optimally oriented faults the value obtained for the friction coefficient existing on such faults is quite within the classical values (0.68), given the pore pressure is in sub hydrostatic conditions. But such a value is only resulting from a gross approximation by a linear trend, which is not consistent with the accuracy on local stress determinations.

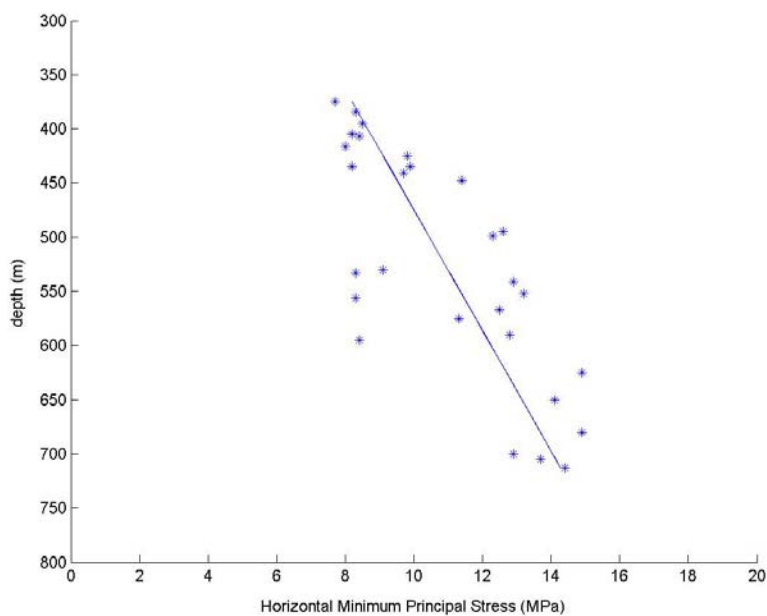


Figure 9: Variation with depth of the minimum horizontal principal stress in Bure (Paris Basin)

Further, at Bure, there is no active fault and, as was shown by the detailed stress measurement campaign, the stress component magnitudes vary according to the rheology of the various sedimentary layers. A nearly zero differential stress has been measured in thick clay-rich layers but larger values have been determined in stiffer, more resistant layers. A somewhat similar behaviour has been documented in the potash mine of the southern Rhine Graben, with a clear influence of the anhydrite content on the differential stress.

Such non linear variation with depth has already been documented in limestone because of the presence of thin lignite beds (Cornet and Burlet, 1992). It has also been documented in volcanic rocks by Haimson and Rummel (1983).

It is concluded here that the smoothing out of stress variations with depth into linear trends may be convenient for gross extrapolation to greater depth. But it should not be taken as a demonstration that vertical stress profiles in sedimentary rocks are governed by friction along optimally oriented faults, given the absence of both microseismicity and actively

creeping fault. It should not be used for integrating together stress tensor components obtained within layers with different rheological characteristics.

For sedimentary formations in very slow deforming zones, the mean slope of the vertical variation trend depends on the rheological characteristics of the various layers as well as on their relative thickness. This may explain the change in slope for the vertical variation of the differential stress above and below the Zechstein salt, in the North German Basin. A more accurate extrapolation method may require a bilinear trend as proposed with equation (2):

$$\mathbf{S}(x) = \mathbf{S}(x_0) + (z-z_0) \mathbf{A}_1 \quad \text{for } z < z_1 \quad (1)$$

$$\mathbf{S}(x) = \mathbf{S}(x_0) + (z_1-z_0) \mathbf{A}_1 + (z-z_1) \mathbf{A}_2 \quad \text{for } z > z_1 \quad (2)$$

Where $\mathbf{S}(x)$ is the stress tensor at point x at depth z , $\mathbf{S}(x_0)$ is the stress tensor at point x_0 at depth z_0 close to the ground surface, \mathbf{A}_1 and \mathbf{A}_2 are second order tensors that represent “mean” vertical stress gradients respectively between z_0 and z_1 and below z_1 where z_1 is located within the Zechstein unit.

5.2. Smoothing out stress directions

According to equations (1) or (2), when eigen vectors of tensors \mathbf{A}_1 , \mathbf{A}_2 and $\mathbf{S}(x_0)$ are not collinear, principal stress directions rotate with depth. This may be helpful for representing rotations observed in the North German Basin. It may also be helpful for mapping principal stress rotations with depth in crystalline formations near the 9km deep KTB site, on the eastern border of Germany (fig. 10). Indeed, in this region the maximum horizontal principal stress direction within the top 1000 m is close to NW-SE (i.e. N135°E) according to Rummel et al. (1983), while according to Brudy and Zoback (1999) it is oriented N 149±15° E around 3000 m, N 166°±17° E between 3000 and 6100 m, N 182°±21° E around 7000 m and N177°±11° E around 7800m.

These rotations of horizontal principal stress directions with depth raise difficulty for mapping horizontal stress orientations. Indeed, when rotation occurs, the depth used for the mapping must be specified. This mapping may be modelled by introducing lateral stress gradients within proper depths intervals in equation (1) or (2). If the objective is not simply to map orientations but to provide approximations of the real stress field, the components of these tensors must satisfy the equilibrium equation within the volume for which the mapping is proposed, i.e.:

$$\text{Div } \mathbf{S} + \rho \mathbf{b} = 0 \quad (3)$$

where \mathbf{S} is the stress tensor, ρ is the equivalent geomaterial density and \mathbf{b} is the body force per unit mass, (i.e. generally simply gravity but may include local perturbations such as flow in porous materials when pressure gradients are high) in any small volume of the domain of interest.

5.3. Interpreting stress fields

One of the motivations for mapping stress fields at different scales is to better understand the origin of these stresses. With this in mind, Heidbach et al. (2010) have derived stress patterns based on the World Stress Map database 2008. They note that short wave length of the stress pattern < 200 km are quite frequent in western Europe” and conclude that second and third-order sources of stress have a major impact” on this stress pattern. This observation is quite complementary to our conclusion that the stress field observed in the Paris Basin is

not related to the local tectonics but rather to presently active local processes that we have proposed to link with regional fluxes.

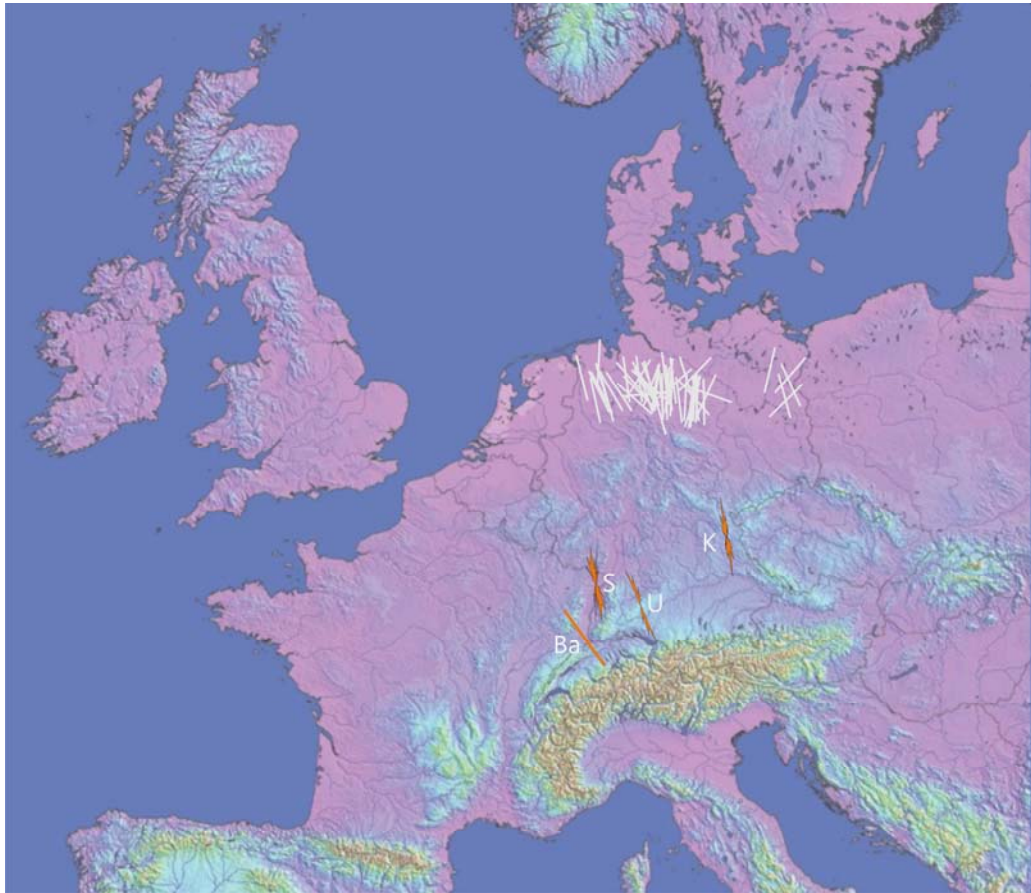


Figure 10. Maximum horizontal principal stress S_H in crystalline rocks (yellow arrows) as compared to S_H orientations from boreholes breakouts in subsalinar boreholes (green, black, red and blue) from the northern German Basin. All data points concern depths greater than 4. km. K stands for 9 km deep KTB borehole, U stands for Urach, S stands for Soultz and Ba stands for Basel. These four sites correspond to data from boreholes deeper than 4 km within the crystalline basement. All the white indicators correspond to breakout orientations below the Zechstein deposit and below 4 km depths.

When only data from boreholes deeper than 4 km in crystalline rocks are considered for the region north of the Alps (figure 10), a global trend in the N160-170°E direction seems to appear, except for the area of Basel where a N140-150°E direction is observed (Valley and Evans, 2009). Interestingly, the inversion of focal mechanisms north of Basel run by Plenefish and Bonjer (1997) is also grossly consistent with the N150° E direction. But these authors note a small rotation from N145°E between 5 and 10 km to N 160°E for depths ranging from 12 to 23 km.

The inversion of focal mechanisms near KTB, in the Eger Rift system, some 80 km to the North East of KTB site, are also consistent with KTB deep stress orientations (Vavricuk, 2002), with the minimum sub-horizontal (20°dip) minimum principal stress oriented N262°E for events located at a depth close to 9 km. This suggests a reasonable continuity of stresses

between 4 and 10 km depths in crystalline formations, quite in contrast to observations in sedimentary basins. Hence the general tendency for a $N160\pm 15^\circ E$ orientation for S_H seems to prevail at depths greater than 4 km for quite a large area, an orientation somewhat different (25° difference) from the NW-SE ($N135^\circ E$) direction often mentioned for North Western Europe when data from all depths are mixed.

The objective of the present paper is not to propose a general interpretation of the regional stress field observed north of the Alps. It is only to outline that data presented in this paper demonstrate that sedimentary formations in areas of very slow deformation rate support stress fields that do not depend only on gravity and on large scale tectonics. Because they host fluids, these sedimentary formations are the site of various solid-fluid interactions that might affect significantly the local stresses and prevent these formations from being efficient markers of deeper tectonic stress fields.

More generally, because sedimentary formations generally include soft materials such as clay, salt, lignite or coal, variations with depth of stress magnitudes are strongly dependent on the creeping characteristics of these materials. In addition, in this type of rock, pressure-solutions and dissolution effects seem also to influence principal stress magnitudes. Hence in domains of very slow deformation rate, sedimentary rocks should not be used as markers of deeper tectonic processes.

Finally, even in domains of crystalline or metamorphic rocks, the stress field is found to rotate with depth in quite a few locations so that maps of the maximum horizontal principal stress direction should always specify the depth range to which they refer.

6. Conclusion

The precise determination of the complete stress tensor at various depths near Bure, in the eastern Paris basin, together with precise data on the variation with depth of the maximum horizontal principal stress orientation in northern Germany, have demonstrated that stress magnitudes in sedimentary formations do not vary linearly with depth. In fact the vertical variations are controlled by the rheological characteristics of the various formations and their relative thickness so that thick weak layers introduce some decoupling between stress field that are active above and below the decoupling zone.

Furthermore, the present existence of a deviatoric stress in the Callovo-Oxfordian argillite in the eastern Paris Basin, suggests that a deformation process is still active today in this region, even though no seismicity is observed and no significant horizontal displacement is detected with GPS monitoring. This has led to hypothesize a local deformation mechanism linked to fluid flow, whether of local or regional scale.

It is concluded that in domains of very slow deformation rates such as northern Europe, local deformation processes in sedimentary formations, whether linked to diapirism or fluid-solid interactions, may influence more significantly the local stress field than does the local tectonic activity.

Finally, because, principal stress directions may rotate with depth in sedimentary rocks as well as in crystalline and metamorphic domains, down to depth much larger than those generally associated with topographic effects, it has appeared necessary to avoid conducting analysis of large scale stress fields without consideration on depth and rock nature.

Acknowledgements

We would like to thank very sincerely Agust Gudmunson for organizing this special volume as a tribute to Jacques Angelier's work on stress fields. We also thank ANDRA for their support concerning the determination and the understanding of the stress field in the eastern Paris Basin. The contribution of Michel Cara, Dominique Bruel and Renaud Toussaint through very fruitful discussions is gratefully acknowledged. Finally we thank F. Roth and J.D Champagnac for their thoughtful reviews of the initial manuscript.

References

- Anderson, R.A., Ingram, D.S., Zanier, A.M., 1973. Determining Fracture Pressure Gradients From Well Logs. *J. Petro. Tech.*, 1259.
- ANDRA, 2009, Référentiel du site Meuse/Haute-Marne, Tome 2; ANDRA report C. RP.ADS. .09.0007 (P. 67) (CRPADS090007.doc).
- Barrio-Alvers, L., Bayer, U., Götze, H.-J., Scheck, M., 1998. Density structure of the Northeast German Basin: 3D modelling along the DEKORP NE-profile, EGS meeting, Nice, France : European Geophysical Society, C 23 p.
- Brace, W.F., Kohlstedt, D.L., 1980. Limits on lithospheric stress imposed by laboratory experiments, *J. Geophys. Res.*, 85. 6248-6252.
- Brudy, M., Zoback M.D., 1999. Drilling induced tensile wall-fractures: Implications for determination of in situ stress orientation and magnitude. *Int. J. Rock Mech. Min. Sci.*, 36, 191-215.
- Cornet, F. H., 2010. Determining the complete stress tensor from Hydraulic Tests: A case history in Sedimentary Rocks from the French Paris Basin; in *Rock Stress and Earthquakes* (ed. Furen Xie), proc. 5th Int. Symp. on in situ Rock Stress, Beijing, China, 77-84, CRC Press, Taylor and Francis.
- Cornet, F. H., Burllet, D. ,1992. Stress field determinations in France by hydraulic tests in boreholes. *J. Geophys. Res.*, 97, B8, 11829 - 11850.
- Economides, M. J., Nolte, K. G., 2003. *Reservoir Stimulation*, pp. 5.1– 5.14, John Wiley, Hoboken, N. J.
- Grote, R., 1998. Die rezente horizontale Hauptspannung im Rotliegenden und Oberkarbon in Norddeutschland,- *Erdöl Erdgas Kohle*, 114, (10) 478-482, Hamburg/Wien (Urban Verlag).
- Grünthal, G. , Wahlström, R., 2003. An Mw based earthquake catalogue for central, northern and northwestern Europe using a hierarchy of magnitude conversions. *J. Seism.*, 7, 507-531.
- Gunzburger, Y., Cornet, F.H., 2007. Rheological characterization of a sedimentary formation from a stress profile inversion; *Geophys. Jou. Int.*; 168, pp 402-418.
- Haimson, B.C., Rummel, F., 1983. Hydrofracturing Stress Measurements in the Iceland Research Drilling Project drill hole at ReydarfJordur, Iceland; *J. Geophys. Res.*, 87, 6631-6649.
- Haimson, B.C., Cornet, F.H., 2003. ISRM Suggested Methods for rock stress estimation; Part III:Hydraulic fracturing methods ; *Int. Jou. Rock. Mech. Min. Sc.*, vol. 40, 7/8, pp 1011-1020.
- Heidbach, O., Tingay, M., Barth, A., Reinecker, J., Kurfess, D., Müller, B.,2010. Global crustal stress pattern based on the world stress Map database release 2008. *Tectonophysics*. 482, 3-15.
- Lefevre, F., Nicoletis, L., Ansel V., Cllet; C., 1992. Detection and measure of the shear-wave birefringence from vertical seismic data; theory and applications. *Geophysics*; 57; no. 11; 1463-1481.
- Müller, B., Zoback, M.L., Fuchs, K., Mastin, L. Gregersen, S. and Pavoni, N., 1992. Regional stress patterns of tectonic stress in Europe. *J. Geophy. Res*, 97 (B8), 11783-11804.
- Nocquet, J.-M., Calais, E., 2004. Crustal velocity field of western Europe from permanent GPS array solutions, 1996-2001. *Geophys. J. Int.*, 15472-88

- Plenefisch, T., Bonjer, K.P., 1997. The stress field in the Rhine Graben area inferred from earthquake focal mechanism and estimation of frictional parameters. *Tectonophysics*, 275, 71-97, Elsevier.
- Röckel, Th., Lempp, Ch., 2003. Der Spannungszustand im Norddeutschen Becken.- Erdöl Erdgas Kohle, 199, Jg. Heft 2, Urban Verlag
- Roth, F., Bäsler, H., Weigold, G., Fuchs, K., Palmer, J., Fleckenstein, P., 1998. Spannungsmessungen in Osteuropa- Orientierungsdaten aus Nordost-Deutschland, Weißrußland und der Ukraine.- ICDP/KTB-Kolloquium, Wissenschaftliches Programm und Abstracts, Bochum
- Roth, F., Fleckenstein, P., 2001. Stress orientation found in north-east Germany differ from the West European trend. *Terra Nova*, 13, 289-296.
- Rutledge, J.T., Phillips, W.S., 2003. Hydraulic stimulation of natural fractures as revealed by induced microearthquakes, Carthage Cotton Valley Gas Field, *Geophysics*, 68, 441-452.
- Rummel, F., Baumgärtner, J., Alheid, H.J., 1983, Hydraulic fracturing measurements along the eastern Boundary of the SW-German Block, in *Hydraulic Fracturing stress Measurements (Zoback and Haimson ed.)*, National Academy Press, Washington D.C., p3-17.
- Savage, W.Z., Swolfs, H.S., Powers, P.S., 1985. Gravitational Stresses in Long Symmetric Ridges and Valleys. *Int. J. Rock Mech. Min. Sc. & Geomech. Abstr.*, 22, 291-302.
- Sileny, J, Hill, D.P., Eisner, L., Cornet, F.H., 2009. Non double couple mechanisms of microearthquakes induced by hydraulic fracturing; *J. Geophys. Res.*, 114, B08307, doi:10.1029/2008JB005987.
- Thiercelin, M.J., Plumb, R.A., 1994. Core-based Prediction of Lithologic Stress Contrasts in east Texas Formations. *Soc. Pet. Eng. Formation Evaluation*, Dec. 1994, 251-258.
- Tingay, M.R.P., Müller, B., Reinecker, J., Heidbach, O., 2006. State and Origin of the Present-Day Stress Field in Sedimentary Basins: New Results from the World Stress map Project. in *proc. 41st US Symp. Rock Mech.(USRMS) (Golden, Colorado, ARMA publ.*
- Toussaint, R., Cornet F.H., 2011. How Chemistry can change stress in anisotropic fractured carbonates ; proceedings of workshop on “Seismic and aseismic deformation in crustal domains subject to very slow deformation rates”
<http://workshopmontstodile.blogspot.com/p/abstract.html>
- Valley, B., Evans K., 2009. Stress Orientation to 5 km depth in the basement below Basel (Switzerland) from borehole failure analysis. *Swiss J. Geosci.*, 102,467-480.
- Vavrycuk, V., 2002. Non-double-couple earthquakes of the January 1997 in West bohemia, Czech Republic: evidence of tensile faulting. *Geophys. J. Int.*, 149, 364-373, doi: 10.1046/j.1365-246X.2002.01654x.
- Wileveau, Y., Cornet, F.H., Desroches, J. and Blümling P., 2007. Complete in situ stress determination in an argillite sedimentary formation.- *Physics and Chemistry of the earth*, 32, 866-878, Elsevier.
- Zang, A.,Stephansson, O, 2010. Stress Field of the earth’s crust (chapt. 11), Springer.
- Zoback, M.D., Barton C.A., Brudy M., Castillo D.A., Finkbeiner T., Grollimund B.R., Moos D.B., Peska P., Ward C.D., Lanyon G.W., 2003,.Determination of stress orientation and magnitude in deep wells; *Int. Jou. Rock. Mech. Min. Sc.*, vol. 40, 7/8, pp 1049-1076.

Table 1 SH orientation from borehole Breakout orientations near Bure, in the Eastern Paris basin; UBI stands for Ultrasonic Borehole Imager

Borehole nb	Geological strata	Logging tool	SH orientation
MSE101	Kimmeridgian	Caliper	N145°E
	Oxfordian limestone	Caliper	N158°E
	Calovo-Oxfordian (COX) Argilite	Caliper	N158°E
HTM102	Lias ans Trias	Caliper	N155°E
EST103	COX Argilite	Caliper	N109°E (uncertain)
EST104	COS Argilite	UBI	N144°±7° E
EST204	COX Argilite	Caliper	N152°±5° E
EST212	COX Argilite	Caliper	N154°±4° E
EST312	Oxfordian limestone	Caliper	N146°±4° E
	COX Argilite	Caliper	N146°±4° E
	Dogger limestone	UBI	N146°±9° E
EST363	Dogger limeCaliperstone	Caliper	N164°±7° E (uncertain)

Table 2 : Orientation (taken from North , positive to the East) of the Maximum Horizontal Principal stress as determined by Hydraulic Fracturing near Bure (Eastern Paris Basin). All depths (in meters) for which HF tests have been conducted are indicated in the left cells, in each of the columns associated to a given borehole. All orientations correspond to vertical fractures seen at the borehole wall. All depths for which a horizontal fracture has been identified are indicated in bold faces. An absence of orientation implies that the fracture was either horizontal or inclined with respect to the borehole axis. Geological strata D refer to Dogger, C1 to lower Callovian, C2 to Callovo-Oxfordian

Underground lab				North East				North-West		Geol. strata	
EST 205		EST 210† EST 209		EST 361		EST 312		EST 413			EST 441
375	173										C3b
384	171										
395	161										
405	154						382	-	520	-	C3a
407	108						389	143	530	149	
416	140								575	144	C2d
435	152								590	154	
441	156						425	158			C2c
							435				
448	155	454			459						
467	156				469				625	150	C2b2
					471				650	136	
471	154				472						
475	154						480		680	155	C2b1
495	125 ?				495		490				
499	161				515						
		531					541	141			C2a
							552	143			
							567	152	700	159	C1
							572	-	705	153	
							576	-	713	146	
							533	142			D4
							556	-			
							595	147			D3
											D2
		703†	155								D1

Table 3. Measurement of the minimum principal stress magnitude as derived from HF tests near Bure (Eastern Paris Basin). Bold numbers correspond to the vertical direction, * refer to the normal stress supported by pre-existing fractures. For the column that includes two boreholes (EST210 and EST209), data relevant to well EST210 are marked by †.

EST 205		EST 210† EST 209		EST 361		EST 312		EST 413		EST 441		Geol. strata
375	7.7											C3b
384	8.3											
395	8.5											
405	8.2							382	-	520	13.8*	C3a
407	8.4							389	14.0/ 10.9*	530	9.1	
416	8.0									575	11.3	C2d
435	8.2									590	12.8	
441	9.7							425	9.8			C2c
								435	9.9			
448	11.4	454	11.5	459	12.0							
467	12.			469	12.0			470	11.0	625	14.9	C2b2
				471	12.5					650	14.1	
471	11.9			472	11.9							
475	12.4							480	11.2	680	14.9	C2b1
495	12.6			495	12.0			490	11.5			
499	12.3			515	12.4							
		531	13.3					541	12.9			C2a
								552	13.2			
								567	12.5	700	12.9	C1
								572	-	705	13.7	
								576	-	713	14.4	
						533	8.3					D4
						556	8.3					
						595	8.4					D3
		655	14.7									D2
		703†	8.3									D1

Tab. 4: Magnitudes of S_{hmin} deduced from suprasalinar layers in boreholes located in the eastern part of the North German Basin.

Borehole	Depth [m]	S_h [MPa]	S_h -Gradient [MPa/km]	S_v [MPa]	Stratigraphy
Angermünde 1/68	1018	> 18,9	> 18,6	22,4	Gipskeuper
Angermünde 1/68	2049,2	31,6	15,4	48,0	Bernburg
Binz 1/73	655	14,2	21,5	14,2	Lias
Dreileben 3/70	61-778,9	> 18,5			Quartär-Basis Zechstein
Feldberg 1/87	2989-4271	> 62,0	> 20,7	70,8	Nordhausen-Werra
Fehrbellin 1/72	1039,9	16,2	15,6	22,0	Wealden K1
Fehrbellin 1/72	990-1070	16,0	16,2		Wealden K1
Fehrbellin 1/72	2836,8	43,2	15,2	64,2	Lettenkeuper
Friedland 1/71	2940	51,7	17,6	69,4	Nordhausen
Friedland 2/70	2029,4	28,7 ??	14,2 ??	46,8	Salinarröt
Gingst 1/73	1346,5	23,7	17,6	31,7	Zechstein, kein Salz
Gorgast 1/70	2165 (-3108)	>44,3 – >61,4	>20,5 – >19,8	51,1	Bernburg (Werra)
Gransee 2/67	54-2175		> 15,2		Quartär-Gipskeuper
Huy-Neinstedt 1/85	553-849,4	11,8-15,7	22,0-18,5	13,7	Volpriehausen- Nordhausen
Kaarßen 1/87	3324-3459	66,9	20,1	82,6	Nordhausen
Kotzen 4/74	1718	22,3	16,8	37,7	Aalenium
Lalendorf 1/75	3460	61,2	17,7	80,9	Nordhausen
Loissin 1/70	1951,4	30,9	15,8	47,2	Nordhausen
Mirow 1/74	2611,2	42,0	16,1	57,9	Schilfsandstein
Mirow 1/74	3728	63,0	16,9	86,1	Solling
Mirow 1/74	3860	65,6	17,0	89,4	Hardeggen
Mirow 1/74	3904	71,1	18,2	90,5	Detfurth
Mirow 1/74	4097	66,5	16,2	95,3	Volpriehausen
Mirow 1/74	4519	74,9	16,6	105,8	Nordhausen
Oranienburg 1/68	1250	> 19,8	> 15,8	30,3	Hardeggen
Otd 1/82	540	9,4	15,4	13,4	Volpriehausen
Pes 233/	2560	37,9-43,6	14,8-17,0	61,9	Nordhausen
Penzlin 1/75	680	15,2	22,3	13,8	Eozän
Penzlin 1/75	3641	66,5	18,3	84,0	Bernburg
Pröttlin 1/81	1995	33,8	16,9	42,7	Lias
Pröttlin 1/81	3100	43,2	15,9	69,7	Detfurth
Rhinow 5/71	2151	31,3	14,5	37,9	Rät
Roxförde 2/62	131,6	2,0	2,67	2,7	Tertiär
Stavenhagen 1/76	3353,6	57,6	17,2	78,2	Hardeggen
Vellahn 1/78	3500		15,2	78,5	Solling
Wesenberg 1/72	1814	39,4	21,7	42,4	Detfurth
Zehdenick 2/75	3813	> 78,6	> 20,6	89,9	Nordhausen

Table 5: Magnitudes of S_{hmin} deduced from salinar layers in boreholes located in the eastern part of the North German Basin.

Borehole	Depth [m]	Sh [MPa]	Sh-Gradient [MPa/km]	Stratigraphy
Angermünde	2401-3577,4	> 50.4 > 75.1	> 21,0	Ohre-Staßfurt
Barth 8	2697,6	54.5	20,2	Staßfurtkarbonat
Barth 9	2644,7	60.8	23,0	Staßfurtkarbonat
Eldena 1/74	3705	79.1	21.1	Ohre
Feldberg 1/87	2989-4271	> 62.0 - 89.4	> 20.7	Nordhausen-Werra
Gingst 1/73	1346,5	23.7	17,6	cont. Zeschstein
Gorgast 1/1a/70	3108,3	>70.0	> 22.5	Staßfurtkarbonat
Greifswald 1/62	2150	43.3	> 20.1	Zechstein
Grevesmühlen	3827-4935,8	>80.4->103.7	> 21,0	Ohre –Werra
Lalendorf 1/75	3777-4168	> 79.7	> 21.1	Aller-Staßfurt
Parchim 1/68	2318,5-4705	> 48.0	> 20,7	Aller-Werra
Peckensen 233/82	3262	79.9	24,5	Werra-Anhydrit
Ramow 11a	3399	65.2	19,2	Staßfurtkarbonat
Pröttlin	3697	> 83,9	> 22,7	Ohre
Schwaan	3426	>77.4	>22,6	Staßfurtkarbonat
Schwerin 1/87	3380,5-5037		>24,0	Friesland-Werra
Wesenberg 1/72	4205,9-2148		>20,4	Bernburg- Werra
Wittenberge 7E/75	1000,5-3776	23,1 – 72, 2	23,1 – 19,1	Salt
Zehdenick	3813-3997	>79.8 - > 83.6	> 20,9	Nordhausen- Werra

Table 6: Magnitudes of S_{hmin} deduced from subsalinar layers in boreholes located in the eastern part of the North German Basin. * Pore pressure estimated

Borehole	Depth (m)	S_{hmin} (MPa)	Shmin effective (MPa)	SV (MPa)	SV effective (MPa)	Shmin-Gradient (MPa/km)	Po* (MPa)
Barth1/63	4469	69.4	19.65	110.7	60.97	15.5	49.7
Barth1/63	5375	87.2	27.34	134.7	74.9	16.2	59.8
Binz 1/73	3163	45.6	10.8	79.2	44.44	14.4	34.8
Boizenburg 1/74	5640.7	85.1	9.3	131.5	55.65	15.1	76.2
Buchholz	2755.15	47.7	17.6	66.6	36.5	17.3	30.1
Eilsleben	990.5	14.5	2.1	24.7	12.3	14.7	12.4
Feldberg 1/87	4288.5	79.6				18.6	
Feldberg 1/87	4888	72.1	11.4	117.1	56.4	14.8	60.7
Friedland 1/71	5079.5	69.9	8.9	123.0	62.0	13.8	61.0
Friedland 1/71	5969.8	79.2	7.6	146.2	74.6	13.3	71.6
Friedland 2/70	3767	53.0	7.37	89.8	44.18	14.1	45.6
Friedland 2/70	5010.3	65.5	4.89	112.1	51.47	13.1	60.6
Gingst 1/73	2047.9	27.6	5.87	49.8	28.06	13.5	21.7
Gingst 1/73	4963.2	68.3	13.71	127.0	71.4	13.8	55.6
Gingst 1/73	6024	81.1	14.87	155.1	88.9	13.5	66.3
Gransee 2/67	5094	78.1	16.0	120.7	58.6	15.3	62.1
Greifswald 1/62	2731	41.6	11.6	65.9	65.9	15.2	30.0
Greifswald 1/62	3836	63.3	21.1	95	52.8	16.5	42.2
Greifswald 1/62	4223	70.1	23.7	105.3	58.8	16.6	46.5
Greifswald 1/62	4275	67.6	20.6	106.7	59.6	15.8	47
Grimmen6/64	2492.1	38.3	10.9	60	32.6	15.4	27.4
Grimmen6/64	3067.5	47.6	13.9	74.8	41.1	15.5	33.7
Grimmen6/64	3616	53.3	13.5	89.1	49.3	14.7	39.8
Grimmen6/64	3923	60.5	17.4	97.1	54	15.4	43.1
Holzhausen	3970	58.4	16	92.5	44.1	16.2	48.4
Jerchel	815	10.6	1.75	19.1	10.0	13.0	9.1
Lalendorf	5276.4	73.7	11.65	125.9	63.89	14.0	62.0
Loissin	4359	61.2-62.5	12.4-13.7	108.1	59.3	13.4-14.3	48.8
Loissin	4713	66.0	13.2	117.5	64.7	14.0	52.8
Loissin	6371	94.3	23.1	162.2	91	14.8	71.2
Oranienburg	4924	72.1	13	121.0	61.9	14.6	59.1
Penkun 1/h2/72	4525	63.2	13.4	106.3	56.6	14.0	49.8
Penkun 1/h2/72	4693.6	61.8	10.2	110.7	59.1	13.0	51.6
Prerow	4460	70.6	17.5	108.3	54.8	15.8	53.5
Prerow	5128	85.3	23.8	126.0	64.5	16.6	61.5
Pudagla	3092.4	46.5	11.9	73.0	41	15.0	34.6
Pudagla	4041.6	59.6	14.3	100.3	55	14.7	45.3
Richtenberg 2/64	2886.3	40.0	8.0	69.7	37.7	13.9	32.0
Richtenberg 3/65	3210	44.8	9.2	78.3	42.7	14.0	35.6
Richtenberg 3/65	4320	60.7	12.9	107.6	59.8	14.1	47.8
Rostock 1/68	4712	71.3	19.9	111.2	60.0	15.1	53.2
Roxförde	1840	26.4	3.3	46.0	22.9	14.3	23.1
Rügen 2/67	2975.8	43.9	10.47	75.5	42.05	14.8	33.4
Rügen 2/67	4293.3	61.2	13.02	99.8	51.64	14.3	48.2
Rügen 4	3188	49.5	13.73	80.2	44.39	15.5	35.8
Sagard 1/70	1518.5	26.3				17.4	
Sagard 1/70	2257	30.0	4.63	56.0	30.7	13.3	25.3
Salzwedel 2/64	3339	55.1				16.5	
Salzwedel 2/64	3341	58.2				17.4	
Salzwedel 2/64	3425	60.5				17.7	
Schadewalde 2/75	1354	19.8	3.7	31.5	15.4	14.6	16.1
Schwerin 1/87	7086	111.4	15.3	172.2	76.1	15.7	96.1
Stavenhagen 1/76	4972	80.6	27.6	119.1	66.11	16.2	53.0
Vellahn 1/1h/78	5347.8	86.7	20.9	124.9	59.13	16.2	65.8
Vellahn 1/1h/78	5637.8	85.9	16.6	132.4	63.1	15.2	69.3
Wesenberg 1/72	4991.4	72.6	12.8	118.7	58.9	14.6	59.8
Zehdenik	5043	74.4	11.92	121.6	59.16	14.7	62.4
Zollchow 1/71	3670	50.5	6.77	87.3	46.74	13.8	43.7
Zootzen	4993	69.7	7.6	119.6	57.5	14.0	62.1

Table 7: Density and vertical stress component vertical gradients for the major lithological units of the North German Basin (after Barrio-Alvers et al. (1998).

Formation	Density [g/cm ³]	vertical stress gradient [MPa/km]
Quaternary + Tertiary	2.10	20.60
Upper Cretaceous	2.13	20.90
Lower Cretaceous	2.30	22.56
Jurassic	2.45	24.04
Keuper	2.56	25.11
Muschelkalk	2.50	24.53
Buntsandstein	2.53	24.83
Zechstein (Upper Permian)	2.15	21.10
Elbe-Folge (Upper Permian)	2.56	25.11
Mirow-Formation (Upper Permian)	2.59	25.41
Parchim-Formation (Upper Permian)	2.59	25.41
Permian Volcanites	2.65	26.00

Tab. 8: Typical pore pressure in boreholes located in the eastern part of the North German Basin

Altmark,	Eastern border	1.11 – 1.26 (g/cm ³).
Ostbrandenburg,	Tuchen depression	1.06 – 1.09 (g/cm ³).
Ostbrandenburg,	Northern border	1.15 - 1.22 (g/cm ³).
Center of the Basin		1.14 - 1.22 (g/cm ³).

Exceptions from these values are found in the center of the basin at the boreholes:

Grevesmühlen 1/78	1.44 (g/cm ³)
Schwaan 1/76	1.35 (g/cm ³).

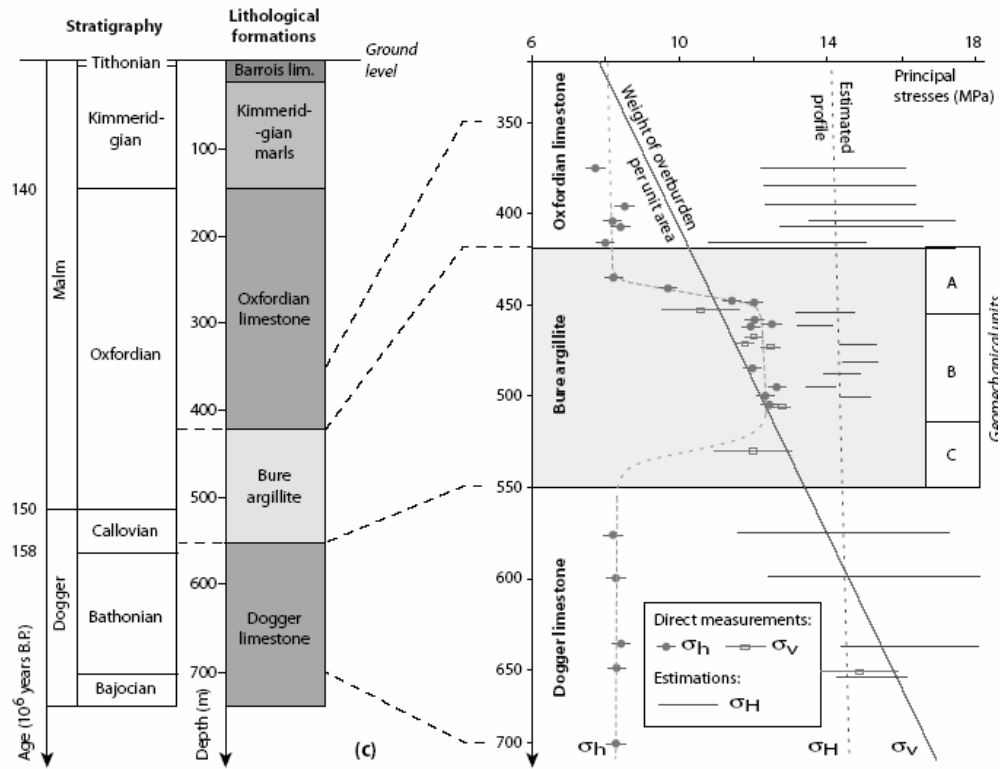
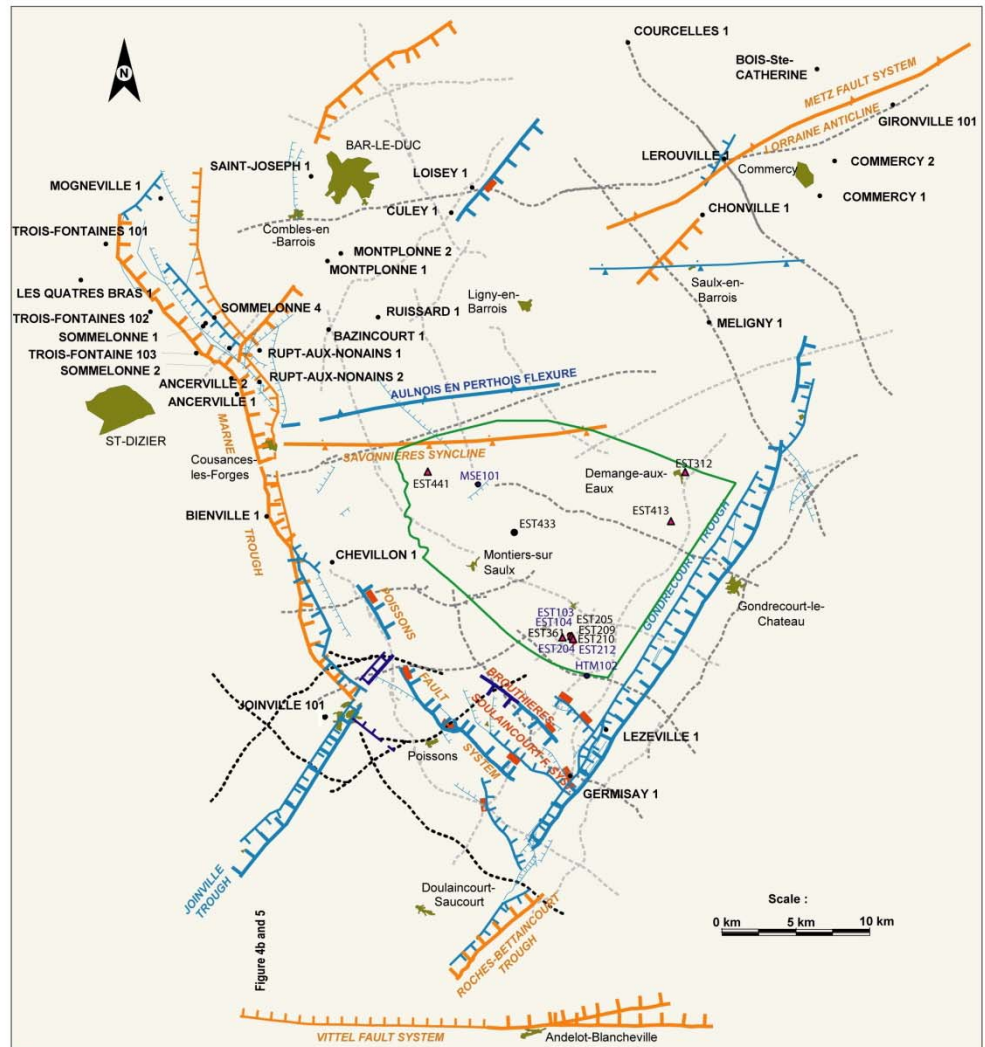
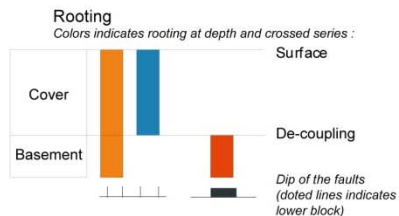


Figure 1. Results from the complete stress determination at the Underground Research Laboratory (URL), in the Eastern Paris Basin (Gunzburger and Cornet, 2007; Wileveau et al., 2007).

Figure 2: Stress observations have been recovered from the various boreholes located within the area delimited by the green contour line, with the URL site located where the density of boreholes is the highest (including EST205). The North East corner includes wells EST312 and EST413, whilst the North West corner includes wells EST441 and MSE2101. Orange coloured structures extend into the basement rock below the sedimentary cover while blue coloured ones remain within the sediments. Stress orientation in the inset is from the present praper.



--- Seismic profiles
 Classification of tectonic features :
 Cartographic extension
 The thickness of the lines indicates :
 — Main (length > 10 km)
 — Secondary (1 < length < 10 km)
 ▲ Andra boreholes
 • Petroleum prospecting boreholes



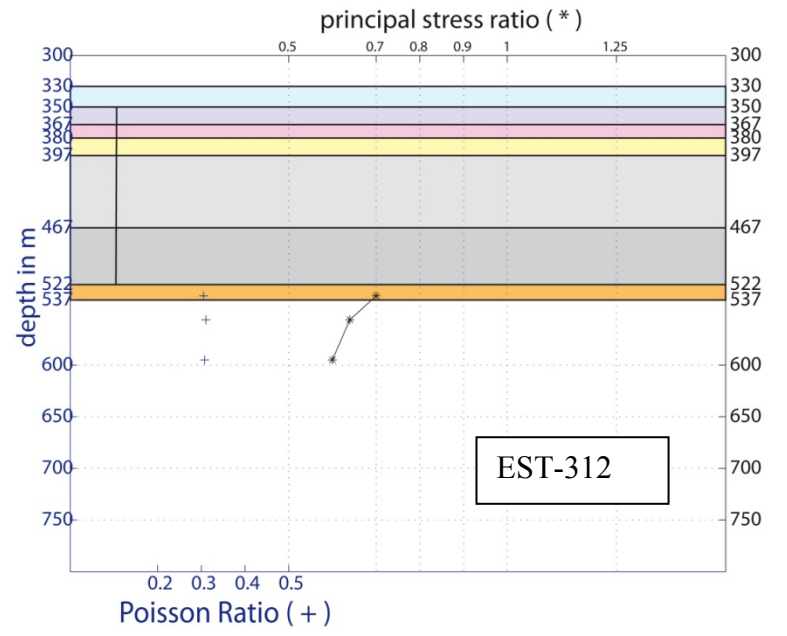
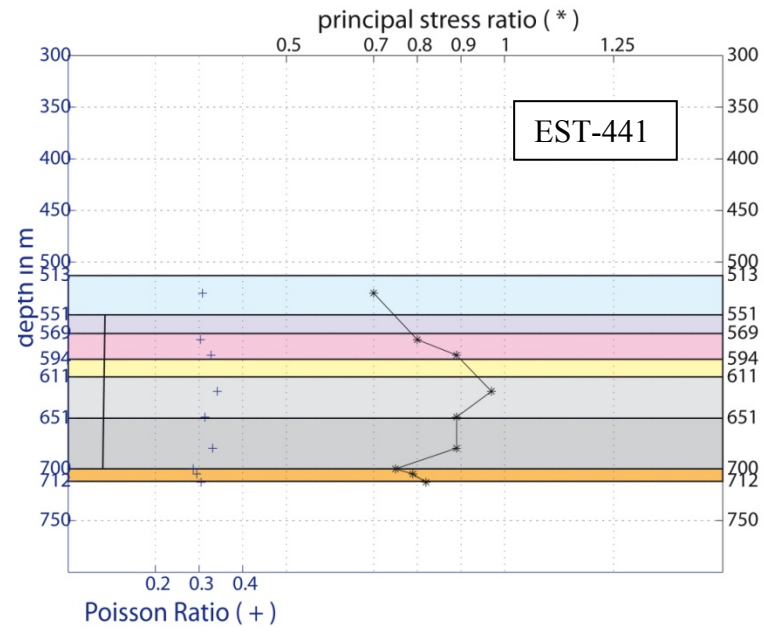
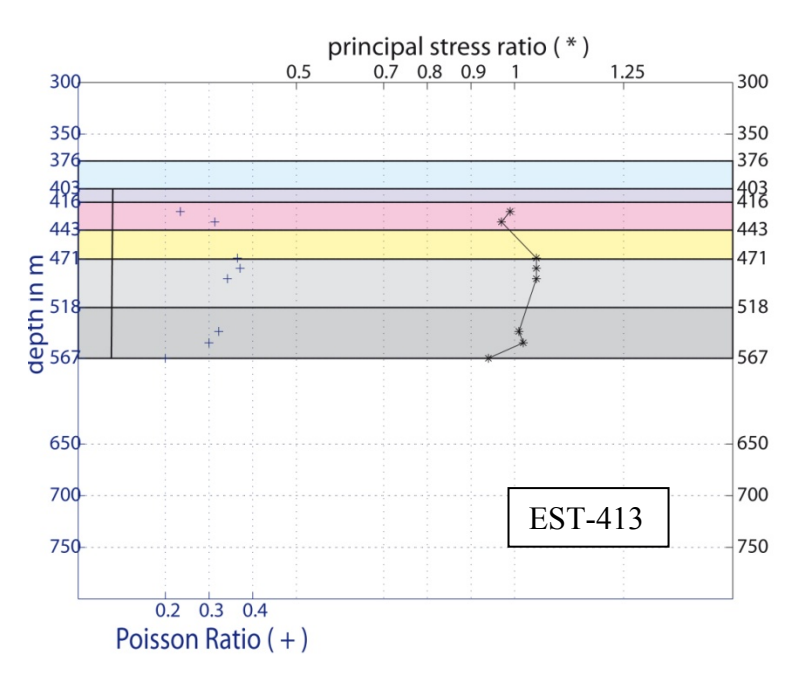
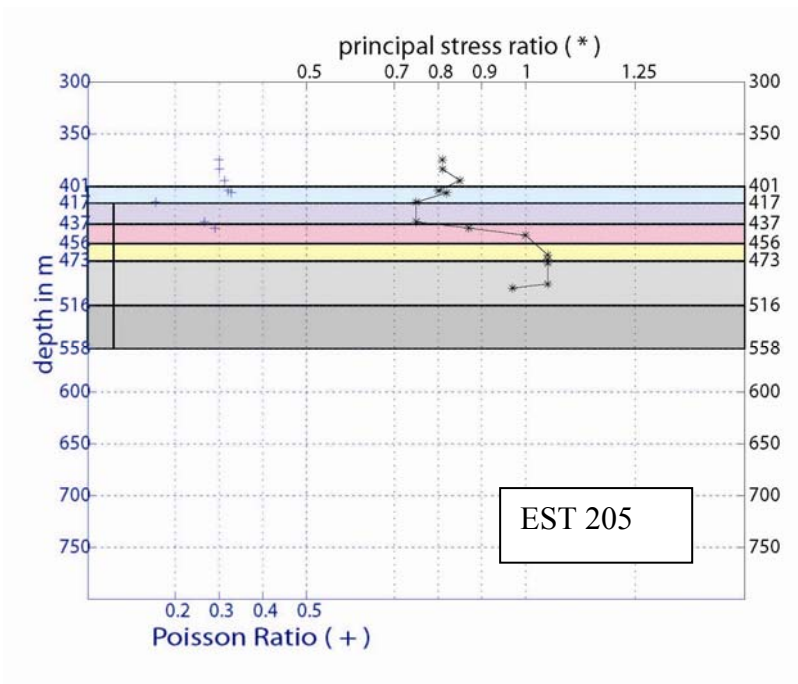


Figure 3. Vertical variation of Poisson's ratio and of the S_H/S_v ratio as a function of the sedimentary structure at the various sites. The vertical line, to the left of each diagram, indicates the COX formation vertical extension. The depth scale is the same for all diagrams so that variability in depth and in thicknesses of the various layers from one borehole to the other may be readily observed. Top left (borehole 205) corresponds to the Underground Research Lab (URL) in the southern corner of the investigated area; Lower left (EST- 441) is located in the North-West corner of the investigated area ; Boreholes EST- 413 and EST-312 are located in the North East corner of the investigated area.

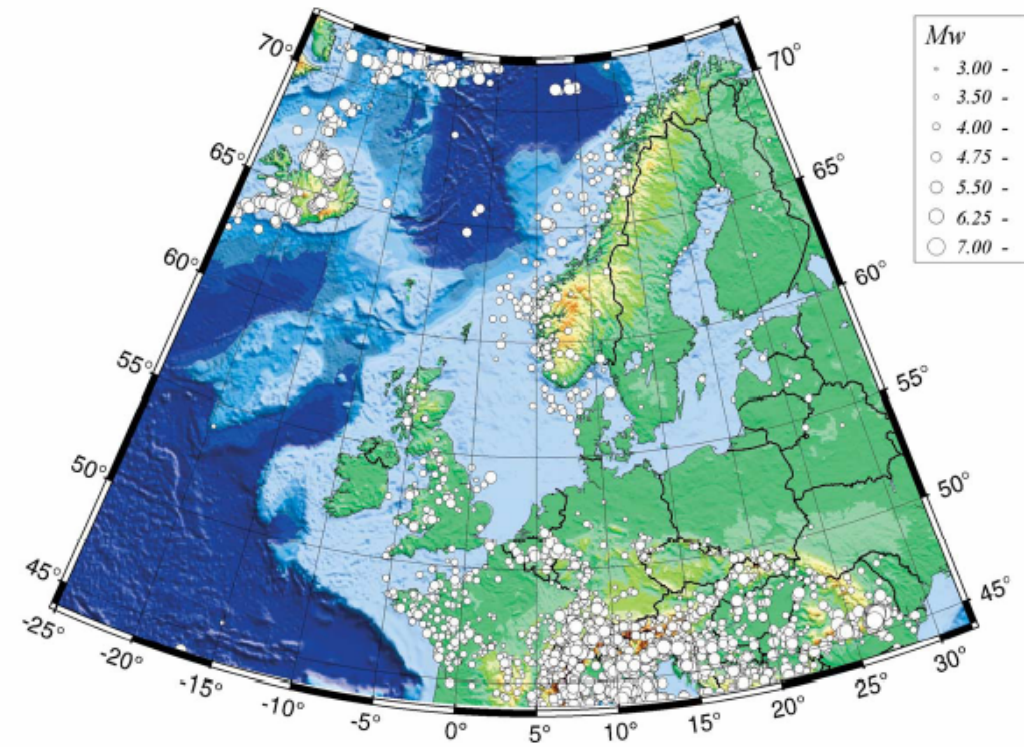
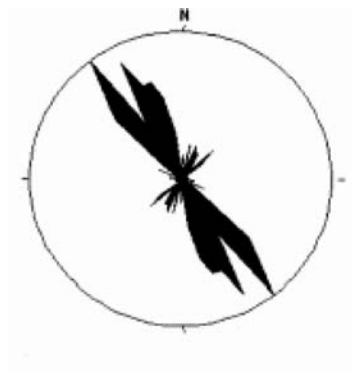
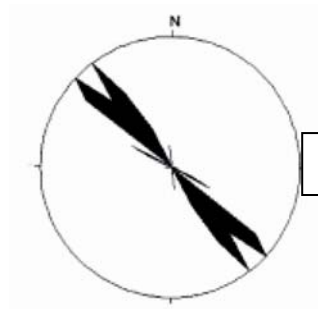


Figure 4. Microseismic activity in North-western Europe from 1300 till 1993 for microseismic events with magnitude M_w larger or equal to 3.5 (adapted from Grünthal and Wahlström, 2003)



219 structures

Strike directions :
10° Classes



21 structures

Strike directions :
10° classes

Figure 5. Orientations of joints and fractures in the Dogger limestone (left) and in the Oxfordian limestone (right). Statistics concern 10° increments in azimuth.

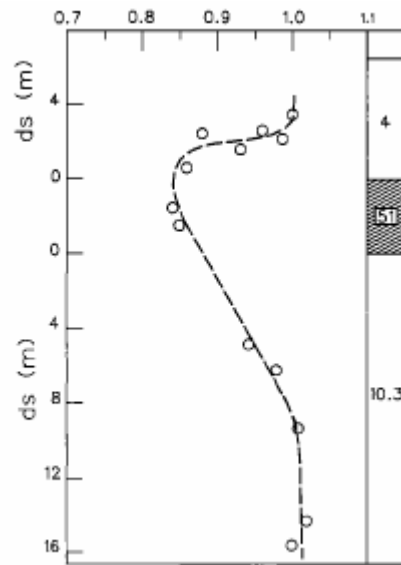


Figure 6 Variation of the S_h/S_v ratio (horizontal axis) as a function of the distance ds (in meters, vertical axis) to layer rich in anhydrite (51%). Numbers in the column to the right indicate the anhydrite content (in percent) in the different layers (after Cornet and Burlet, 1992)

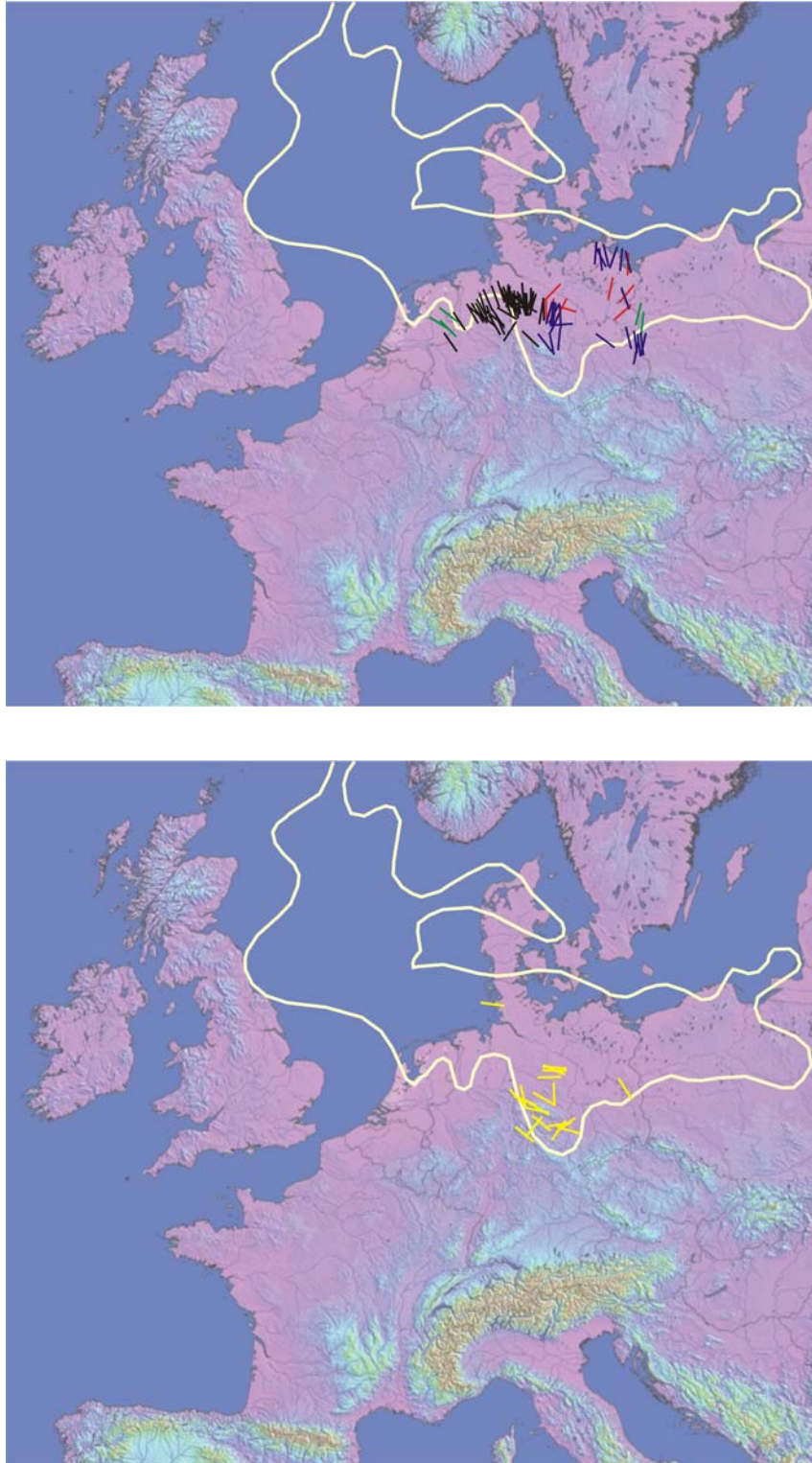


Figure 7. Maximum horizontal principal stress direction. *Top*, sub Zechstein salt data. Data from Grote (1998) are presented as white arrows, from Roth et al. (1998) and from Roth & Fleckenstein (2001) by red arrows, and the data from Röckel & Lempp (2003) are in blue. Stress indicators at the WSM at the border of the Netherlands and Poland are presented in green. *Bottom*, supra Zechstein salt data (from Röckel and Lempp, 2003). The yellow contour indicates the limits of the Zechstein layer

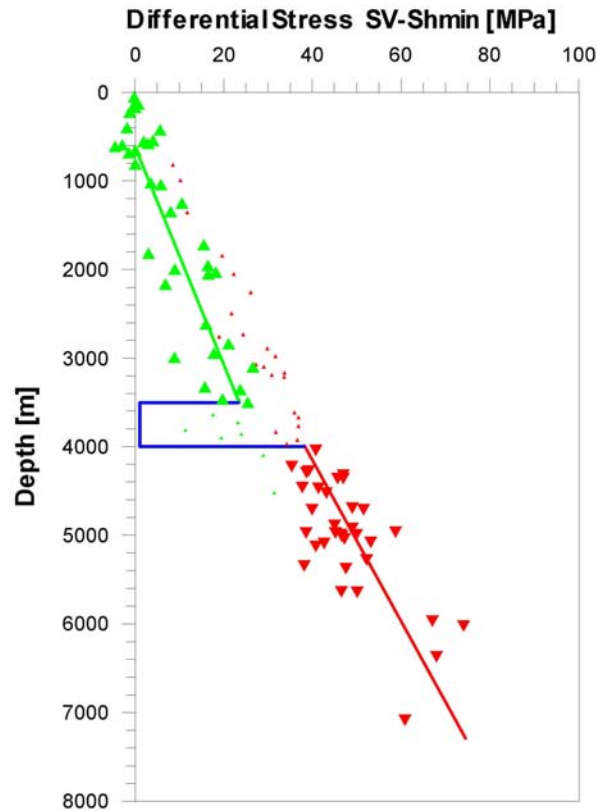


Figure 8 Variation with depth of the (Sv-Sh) differential stress in the Eastern part of the North German basin. The blue notch between 3500 and 4000 m corresponds to the Zechstein evaporitic formation where the differential stress is found to drop for most of the boreholes. The small dots correspond to either subsalt data (green) or suprasalt data (red) from boreholes at locations where the salt is either below or above the mean depth encountered in most of the wells. The gradient of the differential stress in the subsalt is higher compared with the gradient above the salt. Within the salt layer the gradient of the differential stress is close to zero.

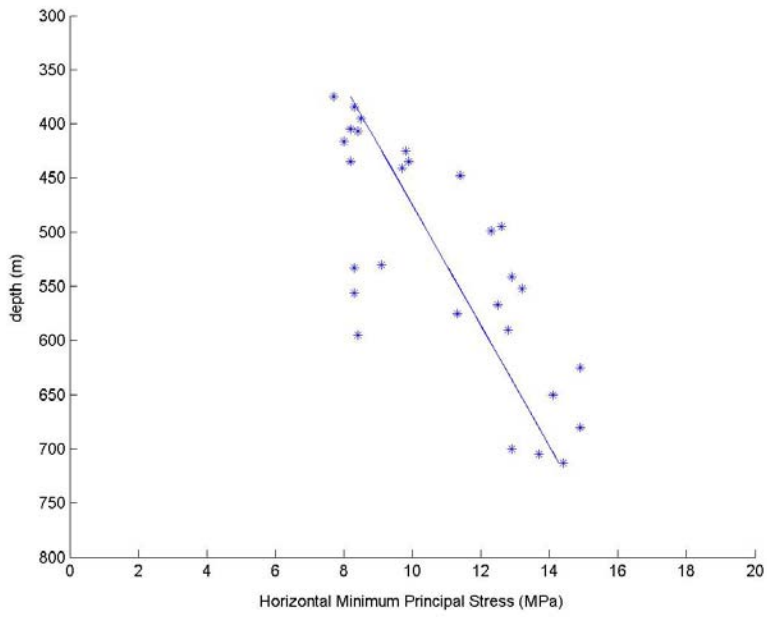


Figure 9 : Variation with depth of the minimum horizontal principal stress in Bure (Paris Basin)

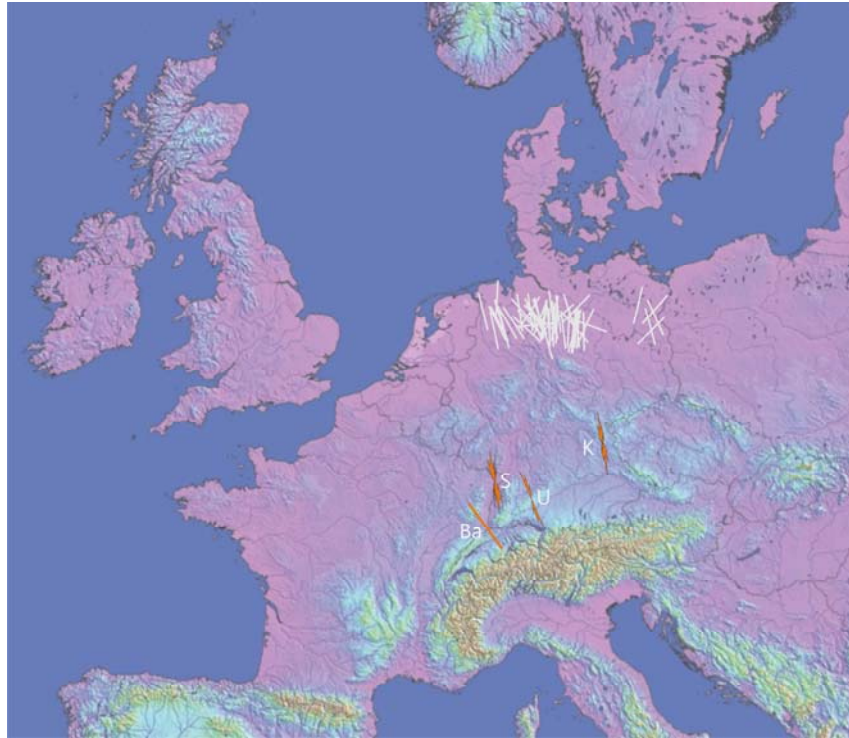


Figure 10. Maximum horizontal principal stress S_H in crystalline rocks (orange arrows) as compared to S_H orientations from boreholes breakouts in subsalinar boreholes (white) from the northern German Basin. All data points concern depths greater than 4. km and sites below the Zechstein deposit. K stands for the 9 km deep KTB borehole, U stands for Urach, S stands for Soultz and Ba stands for Basel.